Mechanisms for Enforced General Acid Catalysis of the Addition of Thiol Anions to Acetaldehyde[1]

H. F. Gilbert and W. P. Jencks*

Contribution No. 1175 from the Graduate Department of Biochemistry, Brandeis University, Waltham, Massachusetts 02154. *Received March 28, 1977*

Abstract: General acid catalysis of the addition of the anion of methyl mercaptoacetate to acetaldehyde exhibits a disappearance or decrease of catalysis at high acid concentrations that is evidence for a change in rate-determining step, a metastable intermediate, and a kinetically significant proton transfer step that traps the intermediate. This catalysis by trapping is enforced by the short lifetime of the anionic addition intermediate, T^- ($k_{-1} = 4 \times 10^7\ s^{-1}$). The more stable intermediates formed from more basic thiol anions exhibit no catalysis and catalysis is enforced for all less stable intermediates. The Brønsted plot for catalysis by trapping is consistent with an "Eigen curve" for proton transfer. However, the Brønsted plot for catalysis of the addition of pentafluorobenzenethiol anion ($pK = 2.7$) has a slope, $\alpha = 0.26$, that is inconsistent with a trapping mechanism and is attributed to catalysis by hydrogen bonding in a preassociation mechanism. Catalysis of the addition of *p*-methoxybenzenethiol anion ($pK = 6.5$) appears to proceed through both mechanisms concurrently, depending on the acidity of the catalyst. Rate and equilibrium constants for the individual steps of the reactions are consistent with the proposed mechanisms. Catalysis by trapping proceeds through a late transition state with complete S–C bond formation ($\beta_{nuc} = 1.0$), whereas catalysis by hydrogen bonding to carboxylic acids involves an early transition state ($\beta_{nuc} \simeq 0.2$). It is shown that the importance of general acid catalysis by hydrogen bonding, relative to the uncatalyzed reaction and to catalysis by trapping, is inversely dependent on the lifetime of the addition intermediate. The value of α increases with decreasing basicity of the attacking thiol anion and β_{nuc} increases with decreasing acidity of the catalyzing acid according to the relationship $\partial\alpha/-\partial pK_{nuc} = \partial\beta_{nuc}/\partial pK_{HA} = 1/c_2 = 0.026$. There is also an increase in β_{nuc} with decreasing thiol anion basicity that probably reflects a later, more basic transition state which forms a stronger hydrogen bond to the catalyzing acid.

The addition of thiol anions to acetaldehyde (eq 1) is a relatively simple reaction that serves to illustrate how different mechanisms of catalysis of addition to the carbonyl group are related to the lifetime of the addition intermediate and the basicity of the carbonyl oxygen atom in the transition state.

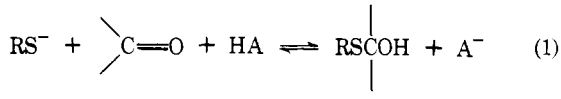

$$RS^- + \text{>C=O} + HA \rightleftharpoons RSCOH + A^- \qquad (1)$$

It has been shown previously that the addition of basic thiol anions exhibits no detectable general acid catalysis,[2] whereas the addition of weakly basic anions of aromatic thiols and thioacetic acid is subject to general acid catalysis with a Brønsted $\alpha \sim 0.2$ (the value of $\alpha = 0.2$ for thiol anion attack corresponds to $\beta = 0.8$ for the reverse, base-catalyzed breakdown of the hemithioacetal).[3] This catalysis has been shown to involve true general acid catalysis rather than the kinetically equivalent specific acid–general base catalysis. The mechanism of catalysis was originally described as being in some sense "concerted", in order to distinguish it from stepwise catalysis by a trapping mechanism.[3] However, it is better described as catalysis in which there has been partial proton transfer from a catalyst that is present in the transition state for attack of the thiol anion.

The experiments described here were initiated because it was noticed that the estimated rate constants for the proton transfer steps of the catalyzed reactions are close to the observed rate constants. This suggested that the proton transfer steps themselves might become kinetically significant or that reaction pathways might exist that avoid the diffusion-controlled proton transfer step, so that it appeared desirable to investigate the relationships between proton transfer, catalysis, and the lifetime of the intermediate anionic addition compound, T^-. The reversible addition of thiols is an unusually simple system because there is no requirement for protonation of the sulfur atom before its expulsion from the addition compounds, so that the rate and equilibrium constants for the individual steps of the overall reaction may readily be calculated from experimental data. In particular, the rate constant k_{-1} for the breakdown of T^-, the anion of the hemithioacetal formed from methyl mercaptoacetate and acetaldehyde (eq 2), was calculated from the estimated pK of the hemithioacetal[4,5] and the known rate constant for its hydroxide ion catalyzed breakdown[3] and was found to be similar to the rate constant k_h for proton abstraction from water by T^- to give TH. This suggested that proton abstraction from water (k_h) is partly rate determining in this reaction and that catalysis of this proton transfer by added buffer acids should increase the observed reaction rate. The results reported here confirm this prediction and show how the progressively decreasing lifetimes of intermediates formed from thiol anions of decreasing basicity lead first to catalysis by trapping and then to catalysis by hydrogen bonding to the developing negative charge on the carbonyl oxygen atom in the transition state through a preassociation mechanism. An additional, unanticipated finding is that the Brønsted coefficient, α, for catalysis by hydrogen bonding increases with decreasing pK of the attacking thiol anion. The simplest explanation of this result is that it is a consequence of a later, more basic transition state with weak nucleophiles.

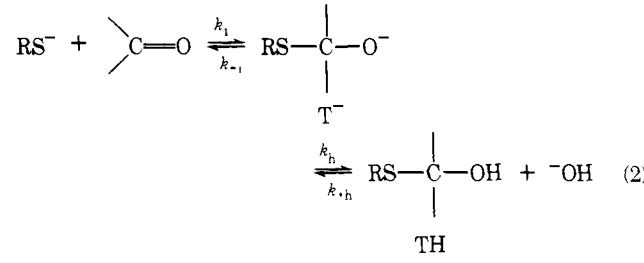

$$RS^- + \text{>C=O} \underset{k_{-1}}{\overset{k_1}{\rightleftharpoons}} RS{-}\underset{T^-}{\overset{|}{\underset{|}{C}}}{-}O^- \qquad (2)$$

$$RS{-}\underset{TH}{\overset{|}{\underset{|}{C}}}{-}OH + {}^-OH \quad \left(\overset{k_h}{\underset{k_{-h}}{\rightleftharpoons}}\right)$$

It has been shown previously that catalysis of the addition of methoxyamine to substituted benzaldehydes occurs through concurrent mechanisms of trapping by general acids and direct catalysis of the addition step by the proton and that the relative importance of these mechanisms for amine additions is determined by the lifetime of the addition intermediate.[6] The concurrent existence of general acid catalysis by trapping and by hydrogen bonding has been observed for the addition of weakly basic carbanions to substituted acetaldehydes.[7] Evidence for catalysis of the addition of weakly basic amines to *p*-chlorobenzaldehyde[5] and formaldehyde[8] by a preassociation

mechanism has been reported and general acid catalysis of these reactions may also involve hydrogen bonding or "concerted" catalysis. Some of the results described here have been summarized in preliminary reports.[9,10]

Experimental Section

Materials. Reagent grade inorganic salts were used without further purification. Organic reagents were redistilled or recrystallized except for trifluoroethanol, methoxyethanol (Aldrich "Gold Label", 99+%), and acetic acid. After distillation, solutions of trifluoroacetone hydrate were found to contain traces of a strongly acidic impurity (<0.7% by titration), which was neutralized with base before preparation of buffers.[11] In a 0.5 M buffer solution, the concentration of the salt of the acidic impurity was $<4 \times 10^{-3}$ M, which would not contribute significantly to the observed catalytic constant. Pentafluoroacetone hydrate was prepared by bubbling pentafluoroacetone gas into cold water. The concentration of pentafluoroacetone hydrate determined by titration with standard base was found to be within 2% of the value determined by weighing the cold water solution before and after addition of pentafluoroacetone.

Acetaldehyde was distilled from sodium bicarbonate under nitrogen. The redistilled acetaldehyde was dissolved in water (degassed with argon) and transferred anaerobically to serum-capped vials that had been filled with argon. Small vials of stock solution (~2 M) were stored at −20 °C and were diluted immediately before use. The concentration of acetic acid was less than 0.04% in this stock solution, as determined by titration. The contribution of this acetic acid to the value of k_{obsd} extrapolated to zero buffer concentration was always less than 5%. The total concentration of acetaldehyde plus hydrate was determined by the absorbance at 280 nm at ionic strength 1.0 M (KCl) using $\epsilon_{280} = 8.55$ M^{-1} cm^{-1} (7.83 M^{-1} cm^{-1} in D_2O).[2] Loss of acetaldehyde by oxidation and evaporation was minimized by storing the stock solution in the reservoir syringes during stopped-flow experiments and by employing Teflon-capped cells for the equilibrium experiments. No significant variation in acetaldehyde concentration was observed during any set of kinetic experiments.

Thiols were stored under nitrogen. Stock solutions of methyl mercaptoacetate were prepared by weight immediately before use. The concentrations of free thiol determined with Ellman's reagent[12] were found to be within 1% of the values determined by weight and decreased by less than 5% during the course of an experiment (approximately 3 h). Stock solutions of other thiols were prepared by volume in 40–100% ethanol immediately before use. All kinetic and equilibrium experiments were performed in random order to minimize any systematic error introduced by loss of thiol or acetaldehyde by oxidation or evaporation.

Equilibrium Constants. Equilibrium constants for hemithioacetal formation at 25 °C and ionic strength 1.0 M (KCl) were measured as described previously with acetaldehyde in large excess over thiol.[3] The acetaldehyde concentration was varied over the range 0.002–0.08 M for *p*-methoxybenzenethiol (9 points), 0.012–0.15 M for 3,4-dichlorobenzenethiol (8 points), and 0.025–0.3 M for pentafluorobenzenethiol (14 points). The thiol concentrations and wavelengths that were used were approximately the same as those for the kinetic experiments. Measurements were made in 0.1–0.3 M hydrochloric acid to avoid ionization of the thiol. The value of K_{hemi} = [hemithioacetal]/[acetaldehyde][thiol] was calculated from $K_{hemi} = K_{obsd}(1 + K_{hyd})(1 + K_{RSH}/a_{H^+})$ where K_{obsd} = [hemithioacetal]/[total acetaldehyde][thiol], K_{hyd} = [hydrated acetaldehyde]/[free acetaldehyde], and K_{RSH} is the ionization constant of the thiol. At 25 °C and 1.0 M ionic strength, $K_{hyd} = 0.85$ for acetaldehyde in water and 0.99 in deuterium oxide.[2]

Equilibrium constants were also determined kinetically for *p*-methoxybenzenethiol and pentafluorobenzenethiol by measuring the pseudo-first-order rate constants for the equilibrium formation of hemithioacetal as a function of acetaldehyde concentration. At least six aldehyde concentrations (0.025–0.2 M) were examined for each thiol. The observed equilibrium constant for hemithioacetal formation (K_{obsd}) is given by the ratio of the slope to the intercept of a linear plot of k_{obsd} against acetaldehyde concentration.[13] The values of the equilibrium constants determined kinetically agreed with the values determined spectrophotometrically within 5–10%.

Kinetics. Kinetics were followed at 25.0 ± 0.1 °C and ionic strength 1.0 M maintained with potassium chloride using a Zeiss PMQII or a Gilford Model 2000 recording spectrophotometer. Reactions with methyl mercaptoacetate were initiated by adding 0.1 mL of 0.5 M acetaldehyde to 3.0 mL of a solution containing buffer and 0.1 M thiol. The disappearance of acetaldehyde was observed at 280 nm. Rate measurements were made in duplicate or triplicate. The reproducibility of the observed rate constants was generally ±2% within a series of runs and variation in different experiments was generally less than 10%.

For reactions with half-lives of less than 5 s, kinetics were monitored with a stopped-flow device designed to fit the cell compartment of the Gilford spectrophotometer.[3] The disappearance of *p*-methoxybenzenethiol was followed at 240 nm after mixing equal volumes of solutions of 0.2 M acetaldehyde and $\sim 10^{-4}$ M thiol, both at ionic strength 1.0 M, to minimize refractive index changes on mixing. The disappearance of 3,4-dichlorobenzenethiol was followed at 245 nm. At pH values less than 2.4, the disappearance of pentafluorobenzenethiol was observed at 230 nm except in chloroacetate buffers where the disappearance of the anion of pentafluorobenzenethiol was observed at 254 nm. Above pH 2.4, the concentration of hemithioacetal at equilibrium is too small to measure absorbance changes accurately, and the decomposition of the hemithioacetal was followed using a pH jump technique.[3] The appearance of pentafluorobenzenethiol anion was monitored at 252 nm. The appearance of *p*-nitrobenzenethiol anion was observed at 410 nm using the pH jump technique.[3] Each rate measurement was repeated at least three times. For reactions with half-lives greater than 10 ms, rate constants could be reproduced within ±2%. For faster reactions, the reproducibility was within ±5–10%.

Rate constants were evaluated from the slopes of plots of log $(A - A_\infty)$ or log $(A_\infty - A)$ vs. time. For reactions with half-lives of greater than 5 s, the plots were linear to greater than 3 half-lives. For stopped-flow measurements, the relatively low precision of the end point read from the oscilloscope trace frequently caused deviation from linearity after 2–3 half-lives.

The pH was determined after a kinetic run by measuring the pH of the effluent from the stopped-flow apparatus or (for methyl mercaptoacetate) the contents of the cuvette using a Radiometer Model 26 pH meter with a GK 2321C glass electrode standardized at pH 4.0 with standard buffer and at pH 1.1 with 0.100 M hydrochloric acid.[14] At low pH values, hydrochloric acid was added to maintain the pH and buffer ratio at constant values.

Treatment of Kinetic Data. The rate constants for hemithioacetal formation from methyl mercaptoacetate and acetaldehyde were determined from the observed rate constants for approach to equilibrium in the presence of excess methyl mercaptoacetate.[2] The rate constants for attaining the hydration equilibrium of acetaldehyde were calculated from the reported catalytic constants[15] and were always at least ten times larger than the rate constant for hemithioacetal formation. Under these conditions, the value of the second-order rate constant for hemithioacetal formation from unhydrated acetaldehyde at constant pH (k_f) is given by[2]

$$k_f = \frac{k_{obsd}K_{hemi}(1 + K_{hyd})}{K_{hemi}[RSH] + 1 + K_{hyd}} \tag{3}$$

The rate constants for the formation of hemithioacetal from thiol anion and acetaldehyde (k_{RS^-}) were calculated from eq 4 where k_+ is the third-order rate constant for the proton-catalyzed addition of free thiol to acetaldehyde.[2]

$$k_{RS^-} = (k_f - k_+a_{H^+})\left[\frac{K_{RSH} + a_{H^+}}{K_{RSH}}\right] \tag{4}$$

The catalytic constants (k_{HA}) for buffer catalysis of the addition of methyl mercaptoacetate anion at low buffer concentrations were evaluated from the slopes of plots made according to[5,16]

$$\frac{k'_{obsd}k_1}{k_1 - k'_{obsd}} = k_{HA}[HA] + \frac{k_ik_1}{k_1 - k_i} \tag{5}$$

where k'_{obsd} is the value of k_{RS^-} corrected for the contribution of the linear catalysis observed at high concentrations of strong acid buffers, k_1 is the limiting rate constant approached at high concentrations of weak acid catalysts, and k_i is the value of k'_{obsd} at zero concentration of buffer.

The value of k_1 was determined from plots of $1/(k'_{obsd} - k_i)$ vs. 1/[buffer]. The intercept of this plot is $1/(k_1 - k_i)$ from which the value of k_1 can be calculated.[5] Calculations were repeated if necessary to provide converging estimates of the values of k_i and k_1. Only data

obtained at less than 0.2 M total buffer concentration were used to estimate the values of k_1, k_i, and k_{HA}.

Equation 6,

$$k_{-1} = k_a[HA]_{1/2}(k_1 - k_i)/k_1 \quad (6)$$

describing the evaluation of k_{-1} from the concentration of buffer required to produce half of the maximum rate increase, $[HA]_{1/2}$, was derived from eq 5. The value of k'_{obsd} observed when half of the maximum rate increase has occurred at $[HA]_{1/2}$ is given by $k'_{obsd} = (k_1 + k_i)/2$. The catalytic constant, k_{HA}, in eq 5 describes the initial slope of a plot of k'_{obsd} against [HA] when k'_{obsd} is much less than k_1. Thus, k_{HA} is the catalytic constant which would be observed if the proton transfer step (k_a) were entirely rate determining and $k_{HA} = k_1k_a/k_{-1}$. Similarly, the rate constant for catalysis by water, $k_w = k_1k_i/(k_1 - k_i)$, is given by $k_w = k_1k_h/k_{-1}$ when proton transfer is rate determing. Substitution of $k_{HA} = k_1k_a/k_{-a}$, $k'_{obsd} = (k_1 + k_i)/2$, and $[HA] = [HA]_{1/2}$ into eq 5 gives eq 6. The catalytic constants for the mechanism exhibiting linear catalysis at high concentrations of strong acid catalysts (k'_{HA}) were evaluated from the slope of the line approached at high buffer concentration after correction of the observed rate constants for salt and solvent effects as described below.

The rate constants for hemithioacetal formation from excess acetaldehyde and aromatic thiols were obtained from

$$k_f = \frac{k_{obsd}(1 + K_{hyd})}{(1 + 1/K'_{obsd})[>C{=}O]_{total}} \quad (7)$$

where $K'_{obsd} = K_{hemi}[>C{=}O]_{total}/((1 + K_{hyd})(1 + K_{RSH}/a_{H^+}))$.[3]

Catalytic constants for the addition of aromatic thiol anions to acetaldehyde were evaluated from the slopes of linear plots of k_{RS^-} against [buffer]. Experiments were performed at two or more buffer ratios except for weak acid buffers which were examined as the free acid, maintaining the pH with a low concentration of hydrochloric acid or an appropriate buffer. The catalytic constants for the general-acid-catalyzed reaction (k_{cat}) were determined from the intercepts at fraction acid = 1.0 of plots of $k_{cat(obsd)}$ vs. fraction acid. The intercepts at fraction acid = 0 did not deviate significantly from zero.

Isotope Effects. Buffer solutions of identical acid-base ratios were prepared in deuterium oxide and water. Acetaldehyde solutions were prepared immediately before use by adding the same volume of freshly distilled acetaldehyde to deuterium oxide and water. The isotopic composition of deuterium oxide solutions was greater than 97% deuterium after the addition of all buffer species. Kinetic and equilibrium measurements were carried out in both deuterium oxide and water on the same day in order to minimize sources of experimental error. The pD of deuterium oxide solutions was obtained by adding 0.40 to the observed pH meter reading.[17] This correction was verified by measurement of the pH and pD of standard solutions of hydrogen and deuterium chloride at ionic strength 1.0 M (KCl).

The observed solvent isotope effect on k_{cat} was corrected for isotope effects on the observed equilibrium constant and for the effects on the ionization of the thiol using eq 8-10

$$\frac{k^H_{cat(RS^-)}}{k^D_{cat(RS^-)}} = \frac{k^H_{(cat)(obsd)}}{k^D_{cat(obsd)}} AB \quad (8)$$

where A represents the correction for the equilibrium effect and B represents the correction for the effect on the ionization of the thiol.

$$A = \frac{[>C{=}O]_T{}^D}{[>C{=}O]_T{}^H} \frac{(1 + K^H{}_{hyd})}{(1 + K^D{}_{hyd})} \left[\frac{1 - \frac{1}{1 + K_{obsd(H)}}}{1 - \frac{1}{1 + K_{obsd(D)}}}\right] \quad (9)$$

$$B = \left[\frac{K_{RSH(H)} + a_{H^+}}{K_{RSH(D)} + a_{D^+}}\right] \frac{K_{RSH(D)}}{K_{RSH(H)}} \quad (10)$$

The pK of p-methoxybenzenethiol, measured spectrophotometrically in deuterium oxide at ionic strength 1.0 M (KCl), was found to be 6.87. The pK of pentafluorobenzenethiol in deuterium oxide at ionic strength 1.0 M (KCl) was taken as 2.98.[18]

Corrections for Salt and Solvent Effects. The observed values of k_{cat} were corrected for solvent and specific salt effects upon the addition of buffers by determining the effects of appropriate model compounds on the observed rate constants. There is necessarily some uncertainty in such corrections, but none of the conclusions of this work are altered if the corrections are omitted. Corrections for carboxylic acid buffers were based on

$$k_{obsd(corr)} = k_{obsd} + \left(\frac{S_A}{100} f_A + \frac{S_B}{100} f_B\right) k_0[buffer]_{total} \quad (11)$$

where S_A is the percent rate depression observed with 1 M acetamide, S_B is the percent rate depression observed with 1 M potassium trifluoroacetate, f_A is the fraction of acid form of the buffer, f_B is the fraction of the basic form of the buffer, and k_0 is the rate constant observed at zero buffer concentration. No correction for solvent and salt effects was made for the buffer-catalyzed reaction. A significant salt or solvent effect on the catalyzed reaction would introduce curvature into plots of k_{obsd} against buffer concentration.[19] No such curvature was observed for catalysis of the addition of the anions of p-methoxybenzenethiol and pentafluorobenzenethiol. Solvent effect corrections for fluoroacetone hydrates and hexafluoro-2-propanol were based on an S_A term determined with 1 M 2-propanol.

Catalytic constants for the addition of pentafluorobenzenethiol anion to acetaldehyde were determined with buffer concentrations of $\leq$0.2 M (except for the upper limit obtained for trifluoroethanol) and did not require correction for salt or solvent effects. Solvent effect corrections on rate constants for the addition of the anion of p-methoxybenzenethiol were generally less than 10% at the highest concentrations of all buffers with pK < 10 and the corrections resulted in less than a 20% change in the value of k_{cat} obtained from uncorrected data. No salt effect corrections were made since plots of $k_{cat(obsd)}$ against f_{acid} were reasonably linear with near-zero intercepts at $f_{acid} = 0$. Larger corrections of k_{cat}, by factors of 1.7 and 2.0, were required for trifluoroethanol and trifluoroacetone hydrate, respectively. Uncorrected values of k_{cat} are shown as the lower limit of the error bars for these catalysts in Figure 7. Salt and solvent effect corrections were made on all rate constants for the addition of methyl mercaptoacetate anion. Corrections on rate constants obtained at less than 0.2 M total buffer concentration were always less than 5% and produced less than a 30% increase in k_{HA}. Corrections at higher concentrations of moderately acidic buffers were $\leq$10% of the observed rate constants and increase the (approximate) values of k'_{HA} by less than 50% for all buffers except acetic acid, for which the increase is approximately 70%. Error limits for the catalytic constants (Table III and Figure 6) include these corrections.

No corrections of the observed rate constant were made for changes in the apparent pH upon buffer dilution.[20] Increasing the concentration of potassium chloroacetate from 0 to 0.75 M at constant ionic strength (1.0 M, KCl) (stock solution adjusted to pH 5.56) in a solution of p-methoxybenzenethiol buffered with 0.05 M acetate buffer (pH 5.56) resulted in no significant change in the concentration of thiol anion (absorbance at 260 nm) although the apparent pH increased from 5.56 to 5.66. The same result was obtained on increasing the concentration of acetamide from 0 to 0.75 M with an increase in pH of 0.05 units.

Calculation of Theoretical Brønsted Plots. The "Eigen curves" for simple proton transfer reactions were calculated from

$$k_{HA} = \frac{K_1k_ak_pk_b}{k_pk_b + k_{-a}k_b + k_{-a}k_{-p}} \quad (12)$$

This steady state rate expression[21] (eq 12) is based on the rate constants shown along the left side and top of Scheme II and fits the curves described by Eigen[22] when $\log k_p\ (s^{-1}) = 10 + 0.5\Delta pK$, $\log k_{-p}\ (s^{-1}) = 10 - 0.5\Delta pK$ ($\Delta pK = pK_{TH} - pK_{HA}$), and $k_{-a} = k_b = 10^{11}\ s^{-1}$.[5] The value of $K_1k_a = k_{HA}$ is the catalytic constant in the region of $\alpha = 0$.

The Brønsted plots describing hydrogen-bonding preassociation mechanisms were calculated from a similar steady state rate law[21]

$$k_{cat} = \frac{(k_{HA} + k'_{HA})k_pk_b}{k_pk_b + (k'_{-1} + k'_{-a})(k_b + k_{-p})} \quad (13)$$

based on an alternative pathway to the $T^-{\cdot}HA$ intermediate with rate constant $k'_{HA} = K_{ass}k'_1$ (Scheme II), and reverse rate constant k'_{-1}. The intercept of the Brønsted plot at $pK_{HA} = 0$ is given by $\log (k_{-1}k_{HA}/k_{-a}) + \alpha(15.74)$.

Assuming that the relative energies of the transition states for proton transfer (k_p, k_{-p}) and diffusion (k_{-a}, k_b) steps are unchanged by hydrogen bonding in the $T^-{\cdot}HA$ and $TH{\cdot}A^-$ intermediates, the ratios k_{-a}/k_p and k_{-p}/k_b do not depend on hydrogen bond stabilization in the intermediates. Substitution of eq 26 into eq 13 and re-

Table I. Equilibrium Constants and Estimated pK Values for Hemithioacetals Formed from Acetaldehyde at 25 °C and Ionic Strength 1.0 M (KCl)

Thiol	pK_{RSH}	K_{hemi}, M^{-1} [a]	pK_{TH} Method I[b]	pK_{TH} Method II[c]	pK_{TH} Method III[d]
Ethanethiol	10.25[e]	36[e]	12.9		
2-Methoxyethanethiol	9.50[e]	32[e]	12.7		
Methyl mercaptoacetate	7.83[e]	60[e]	12.4	11.9	11.7
		53 ± 6[f]			
p-Methoxybenzenethiol (H_2O)	6.49[f]	96 ± 7[f]	12.1	12.8	12.6
(D_2O)	6.87[f]	180 ± 12[f]			
3,4-Dichlorobenzenethiol	5.48[g]	85 ± 8[f]	11.9	12.1	11.8
p-Nitrobenzenethiol	4.57[h]	13[h]	11.7	11.6	11.6
Pentafluorobenzenethiol (H_2O)	2.68[g]	30 ± 3[f]	11.3	11.6	11.7
(D_2O)	2.98[i]	60 ± 6[f]			

[a] K_{hemi} = [hemithioacetal]/[free acetaldehyde][thiol]. [b] Estimated from the pK_a of $HOCH_2CH_2SCH_2OH$ = 12.4 and structure-reactivity correlations.[4,5] [c] Based on the assumption that catalysis by borate represents diffusion-controlled trapping using eq 22, where $k_a = 10^9$ M^{-1} s^{-1}. For weakly basic thiol anions catalysis by borate may be somewhat less than diffusion controlled owing to curvature in the Eigen curves near $\Delta pK = 0$. This effect would cause an overestimation of pK_{TH} by less than 0.3 pK units. [d] Based on the ratio of k_{cat} (borate) to k_0 and a value of $k_{-h} = 10^{10}$ M^{-1} s^{-1} for diffusion-controlled proton transfer between the hemithioacetal and hydroxide ion using eq 23. [e] Reference 2. [f] This work. [g] Reference 23. [h] Reference 3. [i] Reference 18.

Table II. Specific Salt and Solvent Effects on the Rate Constants for the Addition of Thiols to Acetaldehyde at 25 °C[a]

Thiol	Salt or solvent	Buffer	No. of points	Effect on k_{obsd} at 1.0 M salt or solvent, %
Methyl mercaptoacetate	0–0.75 M acetamide	0.011 M HCl	3	−9.5
	0–0.8 M 2-propanol	0.011 M HCl	4	−23
	0–1.0 M Potassium trifluoroacetate	0.011 M HCl	4	−14
	0–1.0 M potassium trifluoroacetate	0.011 M HCl + 1 M acetate 99% acid	3	−16
p-Methoxybenzenethiol	0–0.75 M acetamide	0.05 M acetate 75% acid	5	<−6
	0–0.5 M 2-propanol	0.05 M acetate 75% acid	3	−39
	0–0.5 M 2-propanol	0.8 M acetate 75% acid	3	<−6
Pentafluorobenzenethiol	0–0.25 M 2-propanol	0.01 M acetate 70% acid	2	<+9

[a] Ionic strength was maintained at 1.0 M with potassium chloride.

arrangement leads to

$$k_{cat} = \frac{k_{HA}[k_{-a} + k_{-1}\,\text{antilog}\,[\alpha(15.74 - pK_{HA})]]\,\frac{k_p k_b}{k_{-a}}}{k_p k_b + [k_{-a} + [k_{-1}\,\text{antilog}\,[\alpha(15.74 - pK_{HA})]](k_b + k_{-p})} \quad (14)$$

Results

Equilibrium Constants. Equilibrium constants, K_{hemi}, for the formation of acetaldehyde hemithioacetals of *p*-methoxybenzenethiol, 3,4-dichlorobenzenethiol, and pentafluorobenzenethiol are shown in Table I. Several previously reported values are included for comparison.[2,3] The value of K_{hemi} for hemithioacetal formation from acetaldehyde and methyl mercaptoacetate agrees with the previously reported value.[2] The equilibrium constants vary by less than a factor of 6 and show no trend with changing thiol acidity over the range of thiol pK 2.68–10.25.[3]

The acid dissociation constants of the hemithioacetals were estimated from a measured value[4] of pK_{TH} = 12.4 for $HOCH_2CH_2SCH_2OH$ and structure-reactivity correlations, assuming a fall-off factor of 0.2 for transmission of substituent effects from the thiol to the hydroxyl group.[5] The calculated values of pK_{TH} (method I) are given in Table I, which also includes values obtained from the experimental results by a method that will be described.

Catalysis of Methyl Mercaptoacetate Addition to Acetaldehyde. The rate constants for the addition of methyl mercaptoacetate anion to acetaldehyde increase with increasing concentration of weak acid catalysts, such as boric acid and pentafluoroacetone hydrate, at low catalyst concentrations and level off at higher buffer concentrations after the observed rate has been increased by approximately 25% (Figure 1). With stronger acid catalysts, such as chloroacetic and phosphoric acids, there is a relatively sharp rate increase at low buffer concentrations and a continuing slow increase in rate at higher buffer concentrations. The intercepts of the buffer plots at zero buffer concentration differ because of the increasing contribution of catalysis by the proton at low pH values. Most of the buffer experiments were carried out at pH 2.5, which is convenient for technical reasons. The addition of organic solvents or the substitution of potassium trifluoroacetate for potassium chloride at constant ionic strength causes small decreases in rate at both low and high buffer concentrations (Table II). This indicates that the observed rate increases in the presence of catalysts do not represent solvent or specific salt effects. Similar nonlinear rate increases were observed with all of the buffer catalysts listed in Table III, which includes acids of varying

Table III. Acid-Catalyzed Addition of Methyl Mercaptoacetate Anion to Acetaldehyde at 25 °C and Ionic Strength 1.0 M

Acid	Total buffer, M	pH	No. of points	$10^{-5}k'_{HA}$,[a] $M^{-2}\ s^{-1}$	$10^{-5}k_{HA}$,[b] $M^{-2}\ s^{-1}$
H_3O^+			26	10 ± 4	600 ± 150
Phosphoric	0-0.5	1.90	10	4 ± 2	100[c]
	0-0.5	2.50	10		
Cyanoacetic	0-1.0	1.96	8	1 ± 0.5	64 ± 15
	0-1.0	2.66	8		
Chloroacetic	0-1.0	2.50	10	0.7 ± 0.3	70 ± 30
Acetic	0-0.75	2.57[d]	12	0.3 ± 0.2	50 ± 10
Phosphate monoanion	0-0.5	1.90	10	1 ± 0.5	95 ± 20
	0-0.5	2.50	10		
Hexafluoroacetone hydrate	0-0.7	2.49[d]	12	≤0.1	60 ± 15
Pentafluoroacetone hydrate	0-0.8	2.47[d]	8		55 ± 10
Boric	0-0.5	2.49[d]	12		49 ± 10
	0-0.45	3.05[e]	12		45 ± 10
Hexafluoro-2-propanol	0-0.4	2.48[d]	5		35 ± 6
Trifluoroacetone hydrate	0-1.0	2.54[d]	8		20 ± 8
Trifluoroethanol	0-1.0	2.48[d]	4		<6
Water[f]			26	0.04 ± 0.004	0.045 ± 0.007

[a] Catalytic constants at high buffer concentration (for hydrogen-bonding catalysis). [b] Catalytic constants at low buffer concentration (for trapping, see text). [c] This rate constant represents a rough estimate because of interference from catalysis by the proton and phosphate monoanion. [d] pH maintained with dilute hydrochloric acid. [e] pH maintained with dilute hydrochloric acid and 10^{-3} M methoxyacetate buffer, 71% acid. [f] Experimental second-order rate constants divided by 55.5 M.

structure and charge type, except for the weak acids trifluoroethanol and trifluoroacetone hydrate.

These results provide evidence for a change in rate-determining step with increasing buffer concentration. The catalysis at low buffer concentrations represents catalysis of a step that has a high sensitivity to catalysis. At high buffer concentrations the rate-determining step exhibits no catalysis with weakly acidic catalysts and modest catalysis with stronger acids.

The same change in rate-determining step appears in the pH-rate profile for addition of the thiol in the presence of dilute hydrochloric acid or extrapolated to zero buffer concentration (Figure 2). At low pH the reaction proceeds through the proton-catalyzed addition of the free thiol with the rate constant $k_+ = 1.36\ M^{-2}\ s^{-1}$, which agrees with the previously reported value[2] of $1.40\ M^{-2}\ s^{-1}$. At high pH the rate constants approach a line of slope 1.0, defined by the rate constant k_0, that represents a dependence of the rate on the concentration of thiol anion. At intermediate pH values the rate is faster, by factors of up to 50%, than can be accounted for by the k_+ and k_0 terms. This increase in rate represents catalysis by the proton of the addition of thiol anion that is analogous to the catalysis by other acids of the addition of thiol anion. As shown in Figure 1, the catalysis by the proton is similar to catalysis by other acids in that there is an initial sharp rate increase followed by a break to a smaller rate increase with increasing acid concentration. However, the proton is a more effective catalyst than other acids at both high and low catalyst concentrations.

Catalysis by the proton of the addition of thiol anion appears in the pH-rate profile as a kinetically equivalent pH-independent contribution of the free thiol to the observed rate of reaction. The line with long dashes on the right of Figure 2 represents the sum of the k_0 term and this additional rate increase due to catalysis of thiol anion addition by the proton; it does not include catalysis of addition of the free thiol by the proton (k_+). The sharp rate increase at low proton concentrations, the change in rate-determining step, and the smaller increase in rate at higher proton concentrations that are shown in Figure 1 correspond to the increase in rate above k_0, the break corresponding to the rate constant k_1, and the further increase over k_1 with decreasing pH in Figure 2. The sum of this dashed line and the dashed line for the contribution of k_+ agree with the observed pH dependence of the rate, shown by

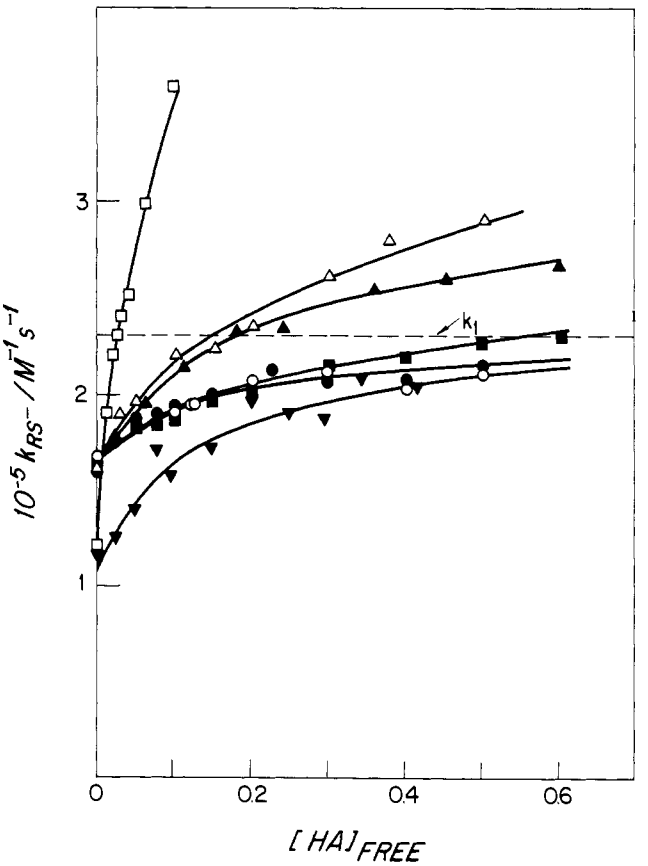

Figure 1. Dependence of the rate constants for hemithioacetal formation from acetaldehyde and methyl mercaptoacetate anion on the concentration of general acid catalysts at 25 °C and ionic strength 1.0 M. The solid lines have been calculated from the catalytic constants k_{HA} and k'_{HA} as described in the Experimental Section and eq 15. (●) boric acid, pH 2.5; (○) pentafluoroacetone hydrate, pH 2.5; (▲) chloroacetic acid, pH 2.5; (△) phosphoric acid, pH 2.5; (■) acetic acid, pH 2.5; (□) the proton; and (▼) boric acid, pH 3.05. The pH was maintained with dilute hydrochloric acid or 0.001 M methoxyacetic acid buffer. The value of k_1 calculated from the data for weak acid catalysts is shown as the dashed line. The points for catalysis by the proton are corrected for the contribution of the k_+ term.

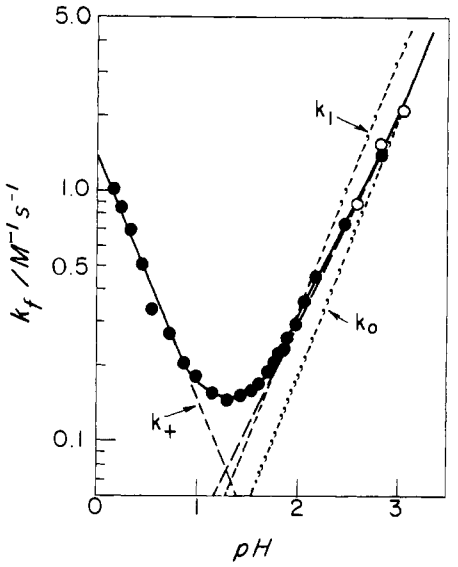

Figure 2. Dependence on pH of the rate constants for hemithioacetal formation from methyl mercaptoacetate and acetaldehyde at 25 °C and ionic strength 1.0 M. The solid line was calculated from the sum of the rate constants described by the lines with long dashes (see text for definitions). Limiting values for the buffer-independent rate constant, k_0, and the rate constant for attack of the thiol anion, k_1, are shown as lines with short dashes. The rate constants were obtained in dilute hydrochloric acid (closed circles) or were extrapolated to zero buffer concentration (open circles).

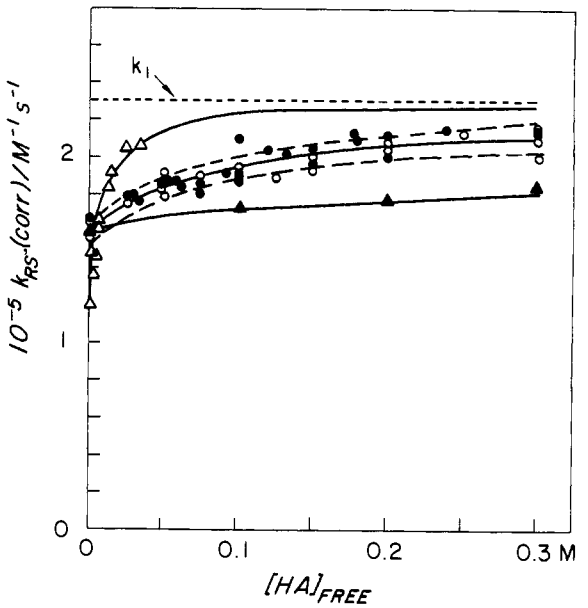

Figure 3. Dependence of the rate constants for hemithioacetal formation from methyl mercaptoacetate anion and acetaldehyde on free acid concentration after correction for catalysis due to k'_{HA}. The points represent catalysis by the proton (△); buffer acids with pK_a less than 4.6 (●); buffer acids with pK_a = 4.6–9.2 (○); and trifluoroacetone hydrate (▲).

the solid line in Figure 2. The observation that the nonlinear rate increase occurs with changing hydrogen ion concentration in the range 10^{-3} to 0.1 M (Figure 1), as well as with a number of other acids of differing structure and charge type at higher concentrations, confirms the conclusion that it is caused by a change in rate-determining step and not by a solvent or specific salt effect.

These results are consistent with the mechanism of Scheme I, in which the upper pathway represents the stepwise forma-

Scheme I

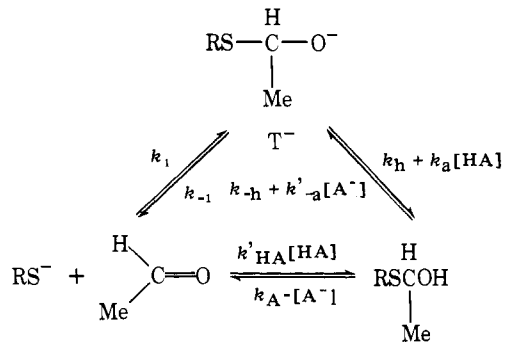

tion of the anionic addition intermediate, T^-, followed by trapping of T^- by proton donation from acids ($k_{HA}[HA]$) and from solvent (k_h), and the lower pathway represents the concurrent general-acid-catalyzed addition of thiol anion ($k'_{HA}[HA]$) that does not proceed through the free intermediate T^-. The observed catalysis proceeds predominantly through trapping of T^- at low acid concentrations and predominantly through the k'_{HA} mechanism at high concentrations of relatively strong acids. The steady-state rate law for Scheme I (in the direction of hemithioacetal formation) is given by

$$k_{RS^-} = \frac{k_1(k_h + k_a[HA])}{k_{-1} + k_h + k_a[HA]} + k'_{HA}[HA] \qquad (15)$$

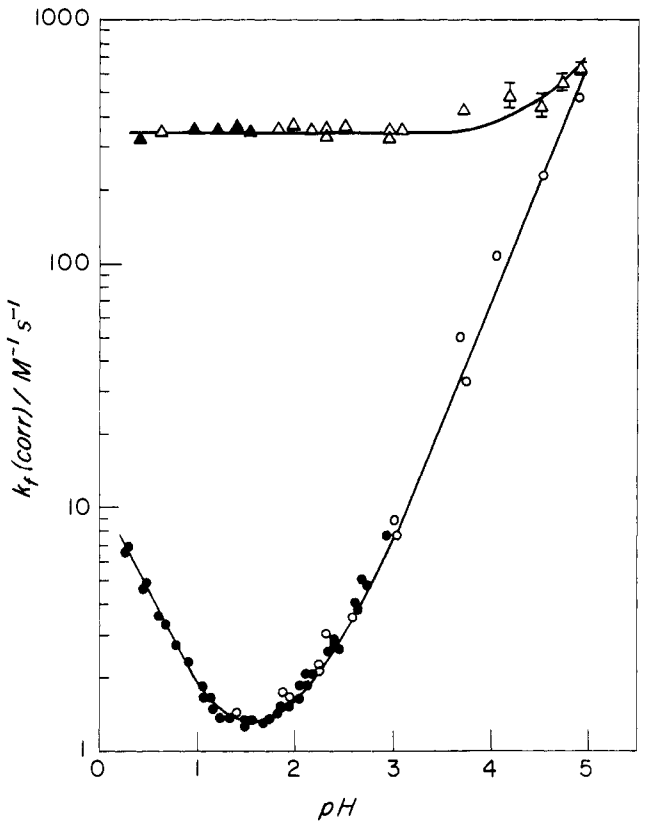

Figure 4. Dependence on pH of the rate constants for hemithioacetal formation from acetaldehyde and pentafluorobenzenethiol (▲) and *p*-methoxybenzethiol (●) at 25 °C and ionic strength 1.0 M. The rate constants for the addition of pentafluorobenzenethiol have been corrected for ionization of the thiol (pK = 2.68). The rate constants were obtained in dilute hydrochloric acid (closed symbols) or were extrapolated to zero buffer concentration (open symbols). Solid lines were calculated from the rate constants in Tables IV and VI.

At high acid concentrations the trapping step ($k_a[HA]$) becomes fast and eq 15 reduces to

Table IV. Acid-Catalyzed Addition of *p*-Methoxybenzenethiol Anion to Acetaldehyde at 25 °C and Ionic Strength 1.0 M (KCl)

Acid	pK_a[a]	Total buffer, M	pH (pD)	No. of points	$10^{-4}k_{cat}$, $M^{-2}\ s^{-1}$
H_3O^+	−1.74			52	220
Difluoroacetic	1.13[b]	0–0.6	1.48	7	19 ± 2
Cyanoacetic (H_2O)	2.31	0–0.75	1.95	7	15 ± 3
(D_2O)	2.78	0–0.5	2.63	5	11
		0–0.4	3.12	5	
Phosphoric	1.89[c]	0–0.46	1.38	6	32 ± 2
		0.1–0.5	1.79	5	
		0.1–0.5	2.37	5	
		0–0.5	4.08[d]	6	
Chloroacetic	2.65	0.05–0.6	2.27	6	9.5 ± 1
		0.025–0.5	3.03	7	
Methoxyacetic	3.36	0.1–0.5	3.03	5	9 ± 1
		0.1–0.5	3.75	5	
Acetic	4.59	0.1–1.0	4.09[d]	8	7.5 ± 0.8
		0.05–0.5	4.58	6	
		0.05–0.5	4.95	6	
Phosphate monoanion	6.55[c]	0–0.46	1.38	6	3.5 ± 1
		0.1–0.5	1.79	5	
		0.1–0.5	2.37	5	
		0–0.5	4.08[d]	6	
Hexafluoroacetone hydrate	6.45[b]	0–0.25	4.09[d]	6	7.4
Pentafluoroacetone hydrate	7.67[b]	0–0.25	4.14[d]	6	4.9
Boric (H_2O)	8.9[e]	0–0.4	4.14[d]	7	4.8 ± 0.8
(D_2O)		0–0.4	4.62[d]	6	5.3
Hexafluoro-2-propanol (H_2O)	9.22[c]	0–0.25	4.12[d]	6	6.2 ± 0.4
(D_2O)		0–0.25	4.62[d]	6	5.6
Trifluoroacetone hydrate	10.45[c]	0–0.5	4.10[d]	6	1.8 ± 0.9
Trifluoroethanol	12.37[f]	0–1.0	4.09[d]	5	1.6 ± 1
Methoxyethanol	14.8[f]	0–1.0	4.12[d]	5	<0.4
Water (H_2O)	15.74			52	0.036
(D_2O)				2	0.020

[a] The pK_a values of carboxylic acids (except difluoroacetic acid) were determined by measuring the pH of a solution of defined ratio of acid and basic components of the buffer, unless noted otherwise. [b] Reference 11. [c] Reference 3. [d] pH maintained with 0.05 M acetic acid buffer, 25% base. [e] Reference 5. [f] Reference 23.

$$k_{RS^-} = k_1 + k'_{HA}[HA] \quad (16)$$

The catalytic constants, k'_{HA}, that describe the linear increase in rate at high acid concentrations are given in Table III. The value of $k_1 = (2.3 \pm 0.2) \times 10^5\ M^{-1}\ s^{-1}$ is given by the limiting rate constant obtained at high concentrations of weak acids, such as boric acid (Figure 1), and agrees with the rate constant obtained by extrapolation of the linear rate increases at high concentrations of the stronger acids to zero buffer concentration.

After correction for the contribution of the k'_{HA} term, the rate constants for catalysis by buffer acids and the proton fall into three groups, as shown in Figure 3. (1) The proton is a considerably more effective catalyst than any of the other acids examined. (2) The rate constants for catalysis by buffer acids of $pK < 4.6$ and of $pK = 4.6$–9.2 are indicated by closed and open circles, respectively, in Figure 3. The fact that there is no significant difference between these two groups of catalysts shows that there is no detectable dependence of catalytic activity on the acidity of the catalyst over this range of acidity. (3) Weak acids with a $pK > 9.2$ are less effective catalysts than the acids in group 2. Approximate rate constants for catalysis by the trapping mechanism, $k_{HA} = k_1 k_a / k_{-1}$, were obtained from the data at buffer concentrations below 0.2 M by correcting the observed rate constants for the change in rate-determining step, as described in the Experimental Section, and are summarized in Table III.

Addition of Aromatic Thiols to Acetaldehyde. The pH–rate profiles for the addition of *p*-methoxybenzenethiol and pentafluorobenzenethiol to acetaldehyde (Figure 4) show that the pH-independent reaction, which corresponds to the proton-catalyzed addition of thiol anion, becomes more important for weakly basic thiols, as has been observed previously.[3] The attack of the thiol anion is catalyzed by buffer acids with no in-

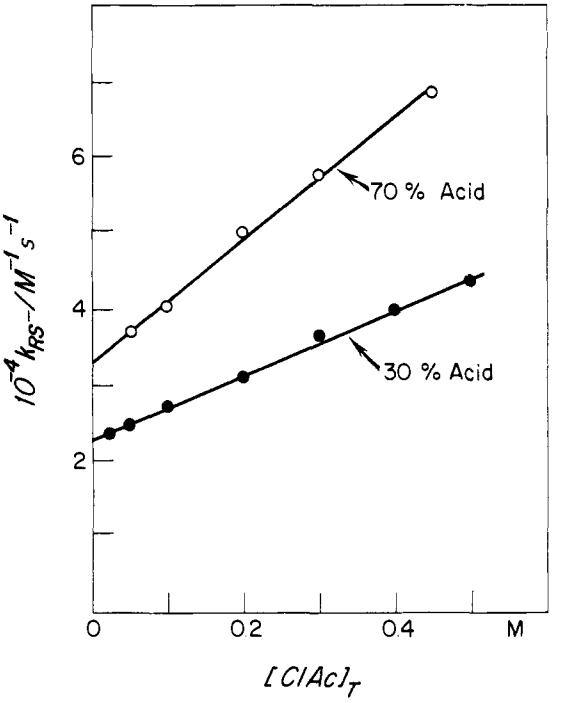

Figure 5. General acid catalysis of the addition of *p*-methoxybenzenethiol anion to acetaldehyde at 25 °C and ionic strength 1.0 M by chloroacetate buffers. (●), 30% acid, pH 2.64; (○), 70% acid, pH 1.94.

Table V. Acid-Catalyzed Addition of 3,4-Dichlorobenzenethiol Anion to Acetaldehyde at 25 °C, Ionic Strength 1.0 M

Acid	Total buffer, M	pH	No. of points	$10^{-4}k_{cat}$, $M^{-2}\ s^{-1}$
H_3O^+			6	120
Cyanoacetic	0-0.4	2.01	5	13 ± 1
	0-0.4	2.69	5	
Boric	0-0.2	4.14[a]	5	2.0
Hexafluoro-2-propanol	0-0.2	4.15[a]	5	2.3
Water			6	0.0026

[a] pH maintained with 0.01 M acetic acid buffer, 25% base.

Table VI. Acid-Catalyzed Addition of *p*-Nitrobenzenethiol Anion to Acetaldehyde at 25 °C, Ionic Strength 1.0 M (KCl)

Acid	Total buffer, M	pH	No. of points	$10^{-4}k_{cat}$, $M^{-2}\ s^{-1}$
H_3O^+				20[a]
Cyanoacetic				2.3[a]
Chloroacetic				1.9[a]
Methoxyacetic				1.4[a]
Acetic				0.65[a]
Boric	0-0.1	4.42[b]	5	0.13
Hexafluoro-2-propanol	0-0.1	4.34[b]	8	0.19
Water				8.3×10^{-5} [a]

[a] Reference 3. [b] pH maintained with 0.01 M acetic acid buffer.

dication of a break at high buffer concentrations nor of buffer catalysis of the addition of the free thiol, RSH. Typical data are shown in Figure 5 and the rate constants for general acid catalysis of the addition of a series of aromatic thiol anions are summarized in Tables IV-VII.

Discussion

Catalysis by Trapping. There is no detectable general acid catalysis of the addition of basic thiol anions to acetaldehyde.[2] The thermodynamically favorable removal of a proton from hemithioacetals by hydroxide ion in the reverse direction (k_{-h}, Scheme I) occurs with a diffusion-controlled rate constant of $k_{-h} = 10^{10}\ M^{-1}\ s^{-1}$.[3] Since the observed rate constant for the hydroxide ion catalyzed breakdown of the hemithioacetal of ethanethiol,[2] $7.3 \times 10^7\ M^{-1}\ s^{-1}$, is smaller than this, the proton transfer step is fast, and the rate-determining step of the breakdown reaction is the expulsion of the thiol anion from the anion of the addition intermediate, T^-, with the rate constant k_{-1} (Scheme I). The proton transfer step in the forward direction involves the abstraction of a proton from water by T^- and the rate constant for this step, k_h, may be calculated from k_{-h} and the equilibrium constant for the proton transfer, according to

$$k_h = k_{-h}K_w/K_{TH} \quad (17)$$

in which K_{TH} is the acid dissociation constant of the hemithioacetal and K_w is the ion product of water. Based on the estimated pK_a for the hemithioacetal of 12.9 (Table I), the value of k_h is approximately $8 \times 10^8\ s^{-1}$. The rate constant for expulsion of the thiol anion from the anionic addition intermediate, T^-, is given by

$$k_{-1} = k_1K_{RSH}/(K_{hemi}K_{TH}) \quad (18)$$

in which K_{RSH} is the acid dissociation constant of the thiol, and is equal to $5.8 \times 10^6\ s^{-1}$. Thus, the intermediate T^- will abstract a proton from the solvent and go on to give the stable hemithioacetal product some 100 times for each time it expels ethanethiol anion and reverts to starting materials. Since proton transfer from the solvent is fast and the attack step is rate determining ($k_h > k_{-1}$) there is no requirement or advantage for catalysis of the proton transfer step by buffer acids

Table VII. Acid-Catalyzed Addition of Pentafluorobenzenethiol Anion to Acetaldehyde at 25 °C, Ionic Strength 1.0 M (KCl)

Acid	Total buffer, M	pH (pD)	No. of points	$10^{-3}k_{cat}$, $M^{-2}\ s^{-1}$
H_3O^+ (H_2O)			20	150
(D_2O)			2	165
Cyanoacetic (H_2O)	0-0.2	1.97[a]	5	11
(H_2O)	0-0.2	2.65[a]	5	
(D_2O)	0-0.2	3.15[a]	5	6.7
Phosphoric[b]	0-0.3	1.38	6	24
	0-0.2	2.28[a]	5	
	0-0.2	3.02[c]	5	
Chloroacetic	0-0.4	2.27	5	8.7 ± 0.5
	0.005-0.2	3.03	5	
Methoxyacetic	0.01-0.05	2.99	5	5.6 ± 0.3
	0.01-0.05	3.73	5	
Acetic	0.01-0.05	3.65	5	2.2 ± 0.2
	0.005-0.015	4.22	5	
	0.005-0.015	4.76	5	
	0.0025-0.0125	4.96	5	
Hexafluoroacetone hydrate	0-0.5	3.02[d]	6	1.1
Pentafluoroacetone hydrate	0-0.05	4.28[e]	5	0.58 ± 0.07
Boric (H_2O)	0-0.2	4.20[f]	5	0.037
(D_2O)	0-0.2	4.71[f]	5	0.028
Hexafluoro-2-propanol (H_2O)	0-0.1	4.23[f]	5	0.29
(D_2O)	0-0.2	4.75[f]	5	0.20
Trifluoroacetone hydrate	0-0.4	4.18[f]	5	0.047
Trifluoroethanol	0-0.8	4.22[f]	5	≤0.0026
Water			4	$3 \pm 1 \times 10^{-5}$

[a] pH maintained with dilute hydrochloric acid. [b] k_{cat} for phosphate monoanion is $\leq 1 \times 10^3\ M^{-2}\ s^{-1}$. [c] pH maintained with 0.01 M methoxyacetic acid buffer, 70% acid. [d] pH maintained with 0.01 M chloroacetic acid buffer, 30% acid. [e] pH maintained with 0.005 M acetic acid buffer, 70% acid. [f] pH maintained with 0.01 M acetic acid buffer, 70% acid.

Table VIII. Estimated Microscopic Rate Constants for Hemithioacetal Formation

Thiol	k_1, M^{-1} s^{-1}	k_{-1}, s^{-1}	k_h, s^{-1}	k_{-h}, M^{-1} s^{-1}	k_a, M^{-1} s^{-1} [a]
Ethanethiol	4.7×10^5 [b]	5.8×10^6 [c]	7.9×10^8 [d]	[e]	
Methoxyethanethiol	4.7×10^5 [b]	2.3×10^7 [c]	5.0×10^8 [d]	[e]	
Methyl mercaptoacetate	2.3×10^5	3.6×10^7 [c] 4.8×10^7 [h]	3.8×10^7 [d] 5.7×10^7 [h]	$6 \pm 4.6 \times 10^9$ [f,g]	3×10^9
p-Methoxybenzenethiol	8×10^4 [i]	1.4×10^9 [c]	3.4×10^8 [d]	$6.7 \pm 0.8 \times 10^9$ [g,j]	2×10^8
3,4-Dichlorobenzenethiol			5×10^7 [d]	$5.6 \pm 2 \times 10^9$ [g]	6.2×10^8
p-Nitrobenzenethiol	7.7×10^3 [i]	6.3×10^9 [c]	3.8×10^7 [d]	9.6×10^9 [k,l]	1.3×10^9
Pentafluorobenzenethiol	3.2×10^2 [i]	1×10^{10} [c]	4.3×10^7 [d]	$1.1 \pm 0.4 \times 10^{10}$ [l]	5.1×10^8

[a] For boric acid; calculated from eq 20, using estimated values of pK_{TH} (method I, Table I). [b] Reference 3. [c] Calculated from eq 18, using average value of K_{TH} from methods II and III (Table I), except for ethanethiol and methoxyethanethiol, where method I was used. [d] Calculated from the observed value of k_{-h} and the average pK_{TH} from methods II and III (Table I) or pK_{TH} from method I and a value of $k_{-h} = 1 \times 10^{10}$ M^{-1} s^{-1} for ethanethiol and methoxyethanethiol using eq 17. [e] Assumed to be 1×10^{10} M^{-1} s^{-1} by analogy with other hemithioacetals for which k_{-h} is rate determining in the hydroxide ion catalyzed breakdown. [f] The large uncertainty results from the correction for partially rate-determining breakdown of T^- in the reverse direction, which depends critically on the error in k_0 and k_1. [g] Calculated from the observed rate constant for approach to equilibrium from the forward direction and the experimental equilibrium constants. [h] Average value calculated from the concentration of H^+ or HA required to reach half of the maximum increase in k_{obsd}, according to eq 6. [i] Estimated from intersection of Brønsted plots for catalysis by hydrogen bonding at $pK_{HA} = 16.0$ times 55.5 M and the statistical factor of 2. [j] The ratio of $k_{-1}/k_h = 4$ suggests that the k_{-1} step is partially rate determining. A correction for partially rate determining k_{-h} from $k_{-h(corr)} = k_{-h(obs)}(1 + k_{-1}/k_h)/(k_{-1}/k_h)$, gives $k_{-h(corr)} = 8 \times 10^9$ M^{-1} s^{-1}. Calculations show that no significant curvature (<4%) in plots of k_{obsd} against buffer concentration at [buffer] < 0.5 M (free acid) is expected if $k_{-1}/k_h = 4$. [k] Reference 3. [l] Rate constant observed experimentally for breakdown of the hemithioacetal.

and no such catalysis is observed. This situation holds generally for the attack of basic thiol anions on acetaldehyde (Table VIII, columns 3 and 4) and for the attack of other strong nucleophiles on unsaturated centers when the initial product is stable enough to be trapped by a proton transfer step involving the solvent before it reverts to reactants.

As the thiol anion becomes less basic, the rate constant k_{-1} for its expulsion from the addition intermediate T^- increases rapidly and the rate constant k_h for proton abstraction from water by T^-, k_h, decreases slightly (Table VIII). An extrapolation of the values of k_{-1} and k_h for more basic thiol anions to the estimated pK of methyl mercaptoacetate suggests that these two rate constants will have similar values for this compound. When k_h and k_{-1} have comparable values some molecules of the intermediate T^- will revert to reactants (k_{-1}) rather than go on to product (k_h) so that both steps are partially rate determining and the addition of a buffer acid that can protonate T^- will increase the observed rate of product formation by trapping T^- to give TH. The rate will increase with increasing buffer concentration until all of the molecules of T^- go on to give hemithioacetal. The attack step, k_1, will then become rate determining and the rate will be independent of buffer concentration.

This behavior is observed for catalysis of the addition of methyl mercaptoacetate anion to acetaldehyde by weak acids such as boric acid and pentafluoroacetone hydrate (Figure 1). The demonstration of a change in rate-determining step of this kind is important because it (a) provides conclusive evidence for a stepwise reaction mechanism with an intermediate, as opposed to a hydrogen bonding, preassociation, or concerted mechanism of catalysis, and (b) provides a "clock" that permits an estimation of the lifetime of the intermediate T^- if the rate constant for the diffusion-controlled trapping of T^- (k_a) can be estimated. The change from a step that is dependent on catalyst concentration to one that is independent of catalyst requires that there be two consecutive transition states in the reaction path, only one of which contains a molecule of acid catalyst. For this simple reaction, this requirement can be met only by a mechanism which involves the formation of T^- in the absence of catalyst in the first step, followed by a proton transfer step that involves diffusion-controlled encounter of T^- with the catalyst, proton transfer, and separation of the conjugate base of the catalyst from TH. This pathway proceeds up the left-hand side and across the top of Scheme II.

Scheme II

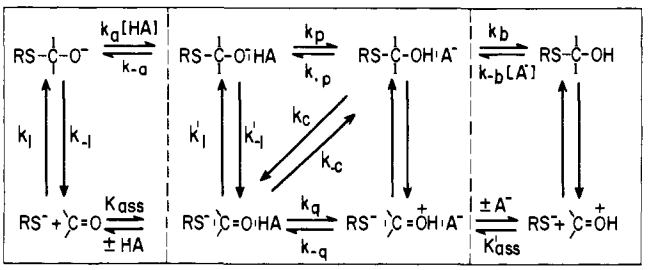

The observation of a change in rate-determining step makes possible an estimation of k_{-1}, the rate constant for breakdown of the addition compound to reactants. In the simplest case, when the "water" reaction is slow, the values of k_{-1} and k_a[HA] are equal at the catalyst concentration, $[HA]_{1/2}$, that causes a half-maximal increase in k_{obsd}, when the change in rate-determining step is half complete and both steps are equally rate determining. In general, the value of k_{-1} is given by eq 6, which is derived in the Experimental Section. Assuming values of $k_a = 10^{10}$ M^{-1} s^{-1} for the proton and 10^9 M^{-1} s^{-1} for other acids,[22] the values of k_{-1} are estimated to be 5.3×10^7 and 4.4×10^7 s^{-1}, respectively, based on the data shown in Figure 3.[24] A similar value of $k_{-1} = 3.6 \times 10^7$ s^{-1} is obtained from the experimentally determined rate constant for thiol anion attack and equilibrium constants (Tables I and VIII) according to eq 18.

Further support for a mechanism of catalysis by trapping comes from the observations, illustrated in Figures 3 and 6, that the catalytic activity is the same within experimental error for all acids in the range of pK = 1.8–9.2. Weaker acids of pK = 10.4–15.7 are less effective, and the proton is approximately tenfold more effective than other acids, as expected from the rapid rate of facilitated diffusion of the solvated proton.[22] Although the small observed rate increases preclude an exact estimation of catalytic constants, the data are adequate for the construction of a Brønsted plot, shown as the upper curved line in Figure 6, which exhibits the characteristics of an "Eigen curve" for a simple proton transfer reaction that is close to diffusion controlled in the thermodynamically favorable direction. The curve is expected to show a break as the proton transfer becomes unfavorable, at approximately the point at which the pK values of the intermediate and catalyst are

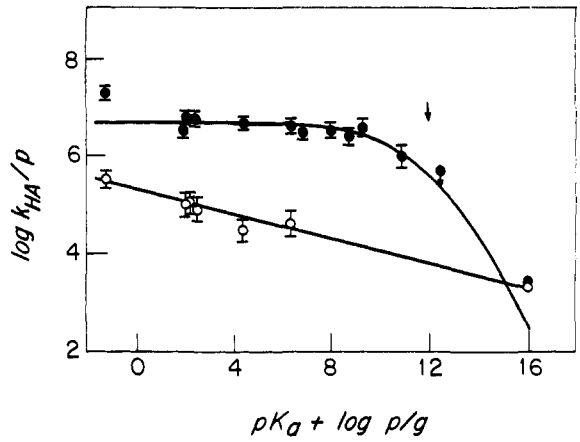

Figure 6. Brønsted plot for general acid catalysis of the addition of methyl mercaptoacetate anion to acetaldehyde at 25 °C and ionic strength 1.0 M. Statistical corrections have been applied to the catalytic constants and the pK_a of the catalysts.[26] For boric acid the values $p = 2$, $q = 4$ were used (see text). The upper line (closed circles) represents rate constants, k_{HA} for catalysis by trapping at low buffer concentrations; the solid line is calculated from eq 12 using $pK_{TH} = 11.9$ (arrow), and $k_{HA} = 4.9 \times 10^6$ M^{-2} s^{-1}. The lower line (open symbols) represents rate constants, k'_{HA} for catalysis by hydrogen bonding, at high buffer concentrations. The line is drawn with $\alpha = 0.13$.

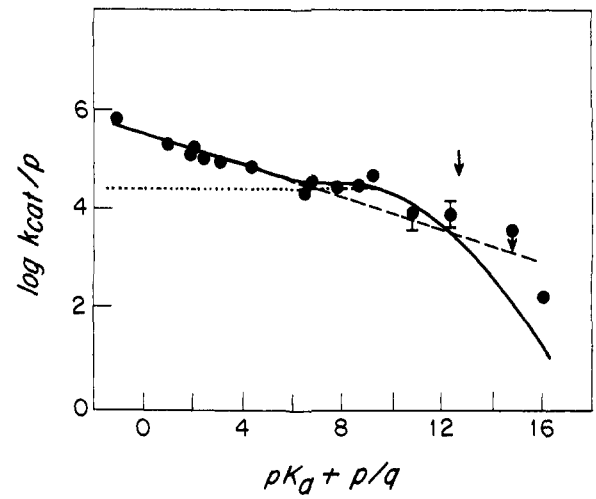

Figure 7. Brønsted plot for general acid catalysis of the addition of *p*-methoxybenzenethiol anion to acetaldehyde at 25 °C and ionic strength 1.0 M. The Eigen curve for diffusion controlled proton transfer (dotted line) was calculated from eq 12 using $pK_{TH} = 12.6$ (arrow) and $k_{HA} = 2.5 \times 10^4$ M^{-2} s^{-1}. The dashed line is an extension of the linear segment of slope $\alpha = 0.16$ observed for the stronger acid catalysts. The solid line was calculated from eq 13 using $k_{-1} = 2.5 \times 10^9$ s^{-1}, $k_{HA} = 2.5 \times 10^4$ M^{-2} s^{-1}, $pK_{TH} = 12.6$ (arrow), and $\alpha = 0.16$. The point for catalysis by methoxyethanol, pK 14.8 represents an upper limit for k_{cat}.

equal.[22] The solid line in Figure 6 is calculated from eq 12, which describes the shape of the Brønsted curves observed by Eigen and co-workers for simple proton transfer reactions,[22] based on a value of $pK_{TH} = 11.9$. The curve gives a satisfactory fit to the data and the position of the break in the curve, based on $pK_{TH} = 11.9$, is consistent with the estimated value of $pK_{TH} = 12.4$ (Table I). The rate constants in Figure 6 are statistically corrected[25] in order to allow comparison with other Brønsted curves; if no statistical correction is made, the fit to the Eigen curve is slightly improved.

The absolute value of the rate constant for protonation of T^- by boric acid, k_a, was calculated from the observed catalytic constant and equilibrium constants and the estimated pK_{TH} (Table I, method I) according to

$$k_{HA} = k_a k_1 / k_{-1} \tag{19}$$

$$k_a = k_{HA} K_{RSH} / K_{hemi} K_{TH} \tag{20}$$

and was found to be 3×10^9 M^{-1} s^{-1}. Since the observed catalytic constants for other acids of $pK = 1.8$–9.2 are essentially the same as that for boric acid (Table III, Figure 3), the rate constants for trapping of T^- by these acids are also close to 10^9 M^{-1} s^{-1}. Similar values were obtained for catalysis by boric acid of the addition of other thiol anions, as shown in the last column of Table VIII. All of these values, with the possible exception of that for *p*-methoxybenzenethiol, are in the range expected for thermodynamically favorable proton transfer from a buffer acid[22] and therefore provide additional evidence for catalysis by the trapping mechanism. The low value for *p*-methoxybenzenethiol is a consequence of the low value of pK_{TH} estimated for this compound (Table I, method I). All of these rate constants, like those for other thermodynamically favorable proton transfers in water (excluding H^+ and OH^-), are significantly below the calculated diffusion-controlled limit for reasons that are not understood;[22,26] however, they are close to this limit and will be referred to as diffusion controlled in this paper.

When the pK of the thiol is decreased further, k_{-1} will continue to increase and a point will be reached at which the proton transfer step is always rate determining ($k_{-1} \gg (k_h + k_a[HA])$), so that there is no change in rate-determining step as the catalyst concentration is increased. This behavior is observed for the reactions with *p*-methoxybenzenethiol anion and all other thiol anions that are less basic than methyl mercaptoacetate anion (Figure 5). The Brønsted plot for the reaction with *p*-methoxybenzenethiol (Figure 7) is similar to the Eigen curve for a trapping mechanism in that there is a break at pK 12.6, close to the estimated pK of the addition intermediate of 12.1, and the catalytic constants of four weak acids show no dependence on acidity, as expected for diffusion-controlled trapping. However, the catalytic constants for stronger acids are larger and the shape of the Brønsted curve is significantly different from that for methyl mercaptoacetate. This suggests that for moderately strong acids some mechanism of catalysis other than the simple trapping mechanism becomes significant for this thiol. The same conclusion is required to explain the continued rate increases at high concentrations of relatively strong acids that are observed with methyl mercaptoacetate (Figure 1).

Catalysis by Hydrogen Bonding and Preassociation Mechanisms. The Brønsted plot for general acid catalysis of the addition of the weakly basic pentafluorobenzenethiol anion to acetaldehyde (Figure 8) has a slope of $\alpha = 0.26$ and is clearly different from the Eigen curve with a limiting slope of zero for diffusion-controlled trapping and from the Brønsted plot for the addition of *p*-methoxybenzenethiol anion (Figures 6 and 7). This slope means that there is significant stretching of the A–H bond and is of the magnitude that is expected if there is hydrogen bonding[28] of the catalyzing acid to the developing negative charge on oxygen in the transition state for the formation of the anionic intermediate T^- (**1**).

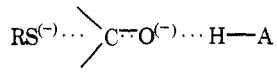

1

Similar, but slightly smaller values of α are found for catalysis of the addition of the more basic anion of 3,4-dichlorobenzenethiol and values of $\alpha \simeq 0.2$ have been reported previously for the anions of benzenethiol, *p*-nitrobenzenethiol, and thioacetic acid.[3]

Catalysis of the addition of methyl mercaptoacetate anion at high concentrations of relatively strong acids, under conditions in which catalysis by trapping is insignificant, also increases with increasing acidity of the catalyst and follows a

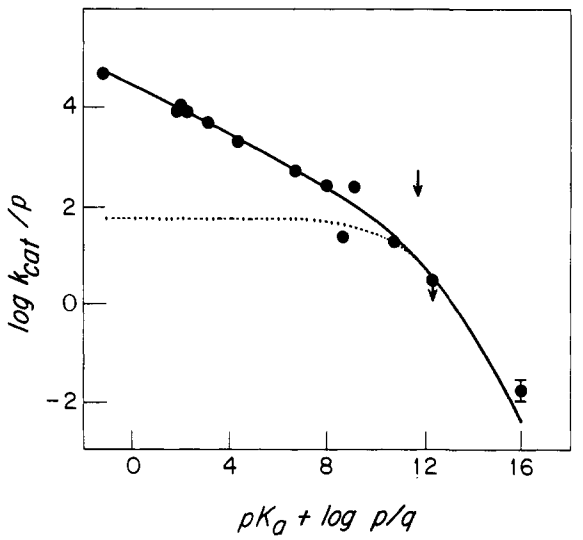

Figure 8. Brønsted plot for general acid catalysis of the addition of pentafluorobenzenethiol anion to acetaldehyde at 25 °C and ionic strength 1.0 M. The Eigen curve for diffusion-controlled proton transfer (dotted line) was calculated from eq 12 with pK_{TH} = 11.8 (arrow) and k_{HA} = 60 M^{-2} s^{-1}. The solid line was calculated from eq 13 and k_{-1} = 6.1 × 10^9 s^{-1}, pK_{TH} = 11.8, k_{HA} = 60 M^{-2} s^{-1}, and α = 0.26.

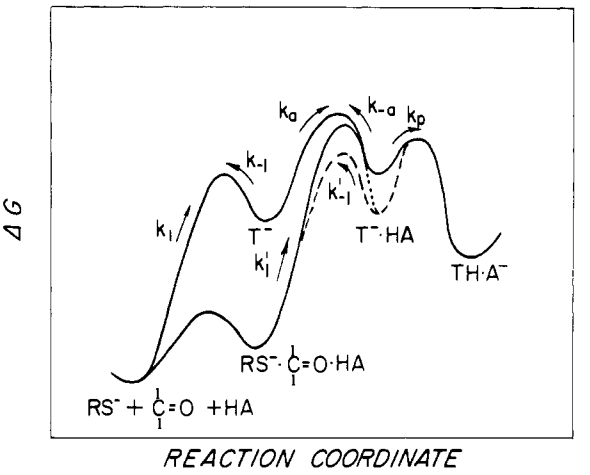

Figure 9. Free energy-reaction coordinate diagrams for a trapping mechanism (upper curve) and a preassociation mechanism (lower curve) with a thermodynamically favorable proton transfer. The perturbations introduced by hydrogen bonding in the transition state for the preassociation mechanism (k'_1, k'_{-1}) and in the T^-·HA complex are shown as dashed lines.

Brønsted line with a slope of α = 0.13 ± 0.03, as shown in the lower line of Figure 6. Comparison of Figures 6, 7, and 8 shows that the catalysis by hydrogen bonding ($\alpha > 0$) becomes progressively more important relative to catalysis by trapping (α = 0) as the basicity of the thiol anion decreases, and represents the predominant mechanism of catalysis of the addition of pentafluorobenzenethiol anion. In Figure 7 the calculated Eigen curve for catalysis by trapping (dotted line) intersects the dashed line of slope α = 0.16 for catalysis by hydrogen bonding at a pK of 7 for the catalyzing acid.

The observed rate constants for catalysis of the addition of pentafluorobenzenethiol anion by carboxylic acids are faster than the rate constants for diffusion-controlled trapping of the intermediate T^-, shown by the dotted line in Figure 8, by factors of up to 100. This means that free T^- cannot be an intermediate in the reaction and that the reaction must proceed through a pathway in which T^- is formed in the presence of the catalyzing acid through a preassociation mechanism.[5,29,30] A preassociation mechanism could occur without stabilization of the transition state for S-C bond formation, with stabilization of the transition state by hydrogen bonding (k'_1, Scheme II), or by a concerted mechanism (k_c, Scheme II). Hydrogen bonding catalysis through a preassociation mechanism involves an initial association of reactants and catalyst in an encounter complex (K_{ass}, Scheme II), S-C bond formation with stabilization of the transition state by hydrogen bonding to HA (k'_1), rapid proton transfer within the T^-·HA complex (k_p), and separation of A^- from TH. This mechanism follows the lower pathway with the dashed line in Figure 9. A preassociation mechanism without hydrogen bonding is shown by the lower solid line. In the reverse direction the addition intermediate breaks down within the T^-·HA complex (k'_{-1}) faster than the catalyst diffuses away (k_{-a}), so that the addition intermediate is not at equilibrium with respect to proton transfer.

The same proton transfer must ultimately occur in a preassociation mechanism as in a trapping mechanism in order to give the neutral hemithioacetal product, and for weak acids this proton transfer, k_p, will become rate determining. For still weaker acids the separation of the complex TH·A^-, with the rate constant k_b, becomes rate determining and the Brønsted plot will approach a slope of −1.0. This is illustrated schematically in Figure 10A, in which the lower line is the Eigen curve

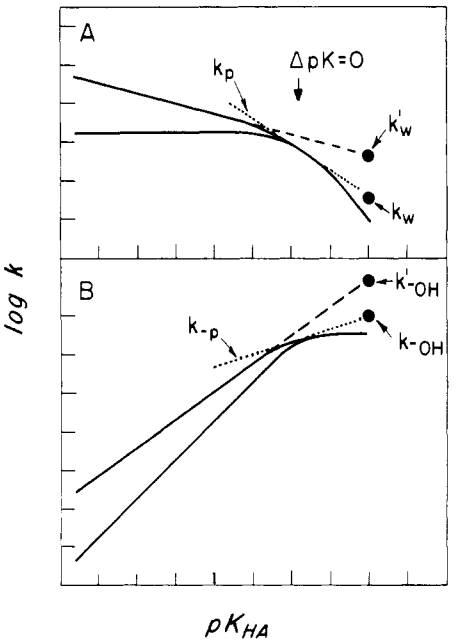

Figure 10. (A) Schematic Brønsted plots for general acid catalysis by a preassociation mechanism with hydrogen bonding ($\alpha > 0$) and trapping (α = 0) for strong acids. The k'_w point is the catalytic constant expected for hydrogen bonding to solvent (k_1/55.5) and the k_w point is the catalytic constant for water through a trapping mechanism. (B) Brønsted plot for the same reaction in the reverse direction expressed as general base catalysis. The k'_{OH^-} point is the catalytic constant expected for hydrogen bonding to hydroxide ion through a preassociation mechanism and k_{OH^-} is the catalytic constant for diffusion-controlled proton abstraction from the product. The rate constant for rate-determining proton transfer (k_p, k_{-p}) in the region near ΔpK = 0 is shown as the dotted line.

for a trapping mechanism, the upper line is the observed Brønsted curve for a preassociation mechanism with hydrogen bonding, and the dashed line is the Brønsted slope that would be observed if the k'_1 step were rate determining for all acids. The dotted line represents the rate constant if the proton transfer step, k_p, is rate limiting, which can be represented approximately[5] by a Brønsted slope of 0.5 for a short distance on either side of ΔpK = 0, and the right-hand part of the curve represents the region in which the separation of A^- and TH is rate determining. In the reverse direction (Figure 10B) this

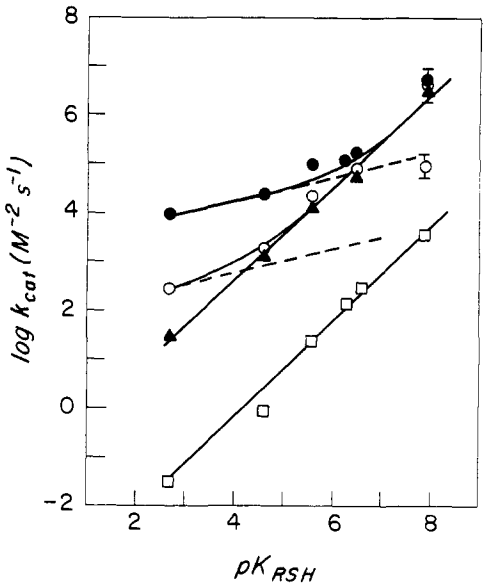

Figure 11. Dependence of the catalytic constants for the general-acid-catalyzed addition of thiol anions to acetaldehyde on the pK_{RSH} of the nucleophile at 25 °C and ionic strength 1.0 M; (●) cyanoacetic acid; (○) hexafluoro-2-propanol; (▲) boric acid; (□) water/55.5 M. The water point for methyl mercaptoacetate is $k_w = k_h k_1/k_{-1}$. The dashed lines are drawn with a slope of $\beta_{nuc} = 0.24$. The value of β_{nuc} for catalysis by water and boric acid is 1.0 ± 0.2.

region represents rate-determining diffusion-controlled encounter of strong bases with TH, for which $\beta = 0$. With weaker bases the proton transfer step, k_{-p}, and then the breakdown of T^- within the T^-·HA complex become rate determining; the latter step is faster than the stepwise reaction pathway that requires dissociation of the T^-·HA complex, shown by the lower solid line. The rate constant for catalysis by hydroxide ion, k_{OH^-}, shows a characteristic positive deviation from the Brønsted line in Figure 10B because of its rapid rate of facilitated diffusion;[22] the same positive deviation is seen for $k_w = k_h k_1/k_{-1}$ in the forward direction (Figure 10A). The rate constants k'_w and k'_{OH^-} for catalysis by hydrogen bonding to water and hydroxide ion are not observed because the slower, diffusion-controlled proton transfer step is rate determining. The ratio k_w/k'_w is equal to k_h/k_{-1} and defines the extent to which proton transfer is rate determining.

The change in the mechanism of catalysis for strong and weak acids with changing pK of the thiol nucleophile is also manifested in structure-reactivity correlations, as shown in Figure 11. Reactions in which trapping is rate determining follow lines of slope $\beta_{nuc} = 1.0 \pm 0.2$. Reactions in which the rate-determining step is nucleophile attack assisted by hydrogen bonding to carboxylic acids and the proton involve only partial formation of the C–S bond in the transition state and show a smaller dependence on the basicity of the nucleophile, with a slope of $\beta_{nuc} \sim 0.2$. The trapping mechanism involves formation of the addition intermediate T^- in a rapid equilibrium step in which the negative charge on the attacking thiol anion is lost, followed by proton transfer and diffusion away of the conjugate base of the catalyst. The effects of polar substituents on the equilibrium addition step are similar to those for protonation of the thiol anion because both reactions involve loss of the negative charge and formation of a covalent bond to the sulfur atom. This accounts for the slope of $\beta_{nuc} = 1.0$ for the reactions involving proton transfer from water and from boric acid in the Brønsted-type correlation of Figure 11. The slope of $\beta_{nuc} \sim 0.2$ for the reactions catalyzed by stronger acids is consistent with catalysis by hydrogen bonding, with a transition state that involves only a partial loss of negative charge on the thiol anion as it attacks the carbonyl group in the rate-determining step (1). For methyl mercaptoacetate, the rate constants for cyanoacetic acid catalysis are known for both the hydrogen bonding and trapping mechanisms. These rate constants fall on the lines of slope 0.2 and 1.0, respectively.

Figure 11 also demonstrates that the importance of catalysis by hydrogen bonding depends on the pK of the acid catalyst. Catalysis by the strong acid cyanoacetic acid proceeds predominantly by the hydrogen bonding mechanism for all thiols of pK < 7 ($\beta_{nuc} = 0.2$). Catalysis by the weaker acids hexafluoro-2-propanol (pK = 9.2) and borate (pK = 9.0) occurs by trapping ($\beta_{nuc} = 1.0$) for all thiols of pK > 2.7. The positive deviation of the rate constant for hexafluoro-2-propanol catalysis of the addition of pentafluorobenzenethiol anion suggests that for this weakly basic thiol, there is catalysis by hydrogen bonding even with weakly acidic catalysts.

For the addition of *p*-methoxybenzenethiol anion, the rate constants for catalysis by trapping and by hydrogen bonding are similar. Thus, the hydrogen bonding and trapping mechanisms are energetically comparable and both mechanisms of catalysis should be observed depending on the pK of the acid catalyst. This is consistent with the positive deviation of the catalytic constants for strong acids above the Brønsted line of slope zero defined by the catalytic constants for weaker acids (Figure 7).

The solvent deuterium isotope effects for the catalyzed reactions are small, in the range expected for catalysis by trapping or hydrogen bonding (Table IX). The small isotope effects for hexafluoro-2-propanol catalysis of methoxybenzenethiolate addition and for boric acid catalysis of both reactions are consistent with diffusion-controlled trapping and the larger isotope effects for hexafluoro-2-propanol catalysis of pentafluorobenzenethiolate addition and for cyanoacetic acid catalysis are consistent with catalysis by hydrogen bonding, but experimental errors and the small rate differences preclude definitive conclusions.

The activity of boric acid as a catalyst is of special interest because boric acid is a pseudoacid that ionizes by extracting hydroxide ion from the solvent rather than by donation of a proton to a base.[27] Boric acid falls on the Brønsted line for catalysis of the addition of the anions of *p*-methoxybenzenethiol and methyl mercaptoacetate. This is consistent with a mechanism of catalysis involving rate-determining proton transfer through an intermediate water molecule. The rate

$$\underset{H}{T^-} + HO + B(OH)_3 \rightleftharpoons \underset{H}{TH} + OB(OH)_3^- \qquad (21)$$

constants for thermodynamically favorable proton transfer to T^- from boric acid (k_a, Table VIII) are close to the rate con-

Table IX. Summary[a] of Solvent Deuterium Isotope Effects for the Acid-Catalyzed Addition of Thiol Anions to Acetaldehyde

Thiol	General acid catalyst	$k_{cat(H)}/k_{cat(D)}$
p-Methoxybenzenethiol	Cyanoacetic	1.34 ± 0.1
	Boric	0.9 ± 0.1
	Hexafluoro-2-propanol	1.1 ± 0.1
	Water	1.8 ± 0.2[b]
Pentafluorobenzenethiol	Cyanoacetic	1.7 ± 0.2
	Boric	1.3 ± 0.3
	Hexafluoro-2-propanol	1.5 ± 0.3
	H_3O^+	0.91 ± 0.15

[a] Data from Tables IV and VII. [b] This isotope effect calculated for the reaction in the reverse direction for the reaction of hydroxide ion with the hemithioacetal using $(k_H/k_D)_{rev} = (k_H/k_D)_{fwd} K^H_{RSH} K^D_w K^D_{hemi}/(K^D_{RSH} K^H_w K^H_{hemi})$ is 1.1, consistent with a diffusion-controlled reaction.[3]

stant of 9.1×10^8 M^{-1} s^{-1} that has been reported for a thermodynamically favorable proton transfer mediated by borate ($\Delta pK = 3.8$).[26] Boric acid is a poor catalyst for protonation of carbon in a vinyl ether and a ketene acetal[31] and borate anion is a poor catalyst for enolization.[32] This is consistent with the conclusion that proton transfer to and from carbon ordinarily does not involve an intermediate water molecule.[33]

On the other hand, boric acid shows a negative deviation of an order of magnitude from the (statistically corrected) Brønsted plot for catalysis of the addition of pentafluorobenzenethiol anion by the hydrogen bonding mechanism (Figure 8). This suggests that boric acid is a poor catalyst for hydrogen bonding to the carbonyl oxygen atom in the transition state of this reaction ($\alpha = 0.26$). Borate also shows a negative deviation from a Brønsted plot for general base catalysis of the addition of 2-methylthiosemicarbazide to *p*-chlorobenzaldehyde, which is thought to proceed through a preassociation mechanism.[5] However, it is a normal catalyst for the acid- and base-catalyzed dehydration of methylene glycol,[25] the addition of urea to formaldehyde,[34] and the acid-catalyzed decomposition of *N*-(*p*-nitrophenyl)carbamate monoanion.[35]

The observed rate constant for boric acid catalysis of pentafluorobenzenethiolate addition sets an upper limit for catalysis of this reaction by trapping. The fact that this rate constant falls on the line for catalysis by trapping ($\beta_{nuc} = 1.0$) in the structure–reactivity correlation of Figure 11 suggests that the observed rate constant actually represents catalysis by the trapping mechanism.

The dissociation constants of the hemithioacetals may be calculated from the observed rate constants for catalysis by boric acid according to

$$K_{TH} = K_{RSH}k_{cat}/(k_aK_{hemi}) \qquad (22)$$

if it is assumed that this catalysis represents rate-determining trapping with a rate constant $k_a = 1 \times 10^9$ M^{-1} s^{-1}. The resulting values of pK_{TH} are shown in Table I, method II. These dissociation constants can also be calculated from the ratio of the observed rate constants for catalysis by boric acid, which represents thermodynamically favorable proton transfer, and by water, which represents thermodynamically unfavorable proton transfer, according to

$$K_{TH} = \frac{k_{cat}k_{-h}K_w}{k_wk_a} \qquad (23)$$

The results, based on a value of $k_{-h} = 1 \times 10^{10}$ M^{-1} s^{-1}, are shown in Table I, method III. These calculated values agree with each other and with values calculated from a measured dissociation constant[4] and structure–reactivity correlations,[5] using a fall-off factor of 0.2 (Table I, method I), except for moderate deviations for the hemithioacetals of methyl mercaptoacetate and *p*-methoxybenzenethiol. Factors that may contribute to these deviations include the relatively large experimental error for the methyl mercaptoacetate reaction and a difference between the structure–reactivity behavior of aliphatic and aromatic thiols caused by resonance stabilization of substituted benzenethiol anions.

Requirements and Advantages for Mechanisms of Catalysis. General acid catalysis is commonly observed for the addition of weakly nucleophilic reagents to the carbonyl group, whereas the addition of strong nucleophiles to reactive carbonyl compounds is usually uncatalyzed.[36] The addition of thiol anions to acetaldehyde provides an example of this behavior and illustrates how the mechanism and importance of general acid catalysis are determined by the properties of the reactants and intermediates. In this section we will describe how the importance of general acid catalysis by hydrogen bonding is directly proportional to the rate constant, k_{-1}, for breakdown of an unstable addition intermediate T^- to reactants, as well as to the strength of the hydrogen bond between HA and the transition state. The different mechanisms for the addition reaction are defined in Scheme II.

Enforced general acid catalysis by trapping *must* appear whenever the rate constant for breakdown of T^- to reactants, k_{-1}, becomes larger than the rate constant for conversion of T^- to TH by proton abstraction from water, k_h. Thus, the appearance of catalysis by trapping depends directly on k_{-1}/k_h. When $k_h \ll k_{-1}$ (proton transfer is rate determining), the advantage of catalysis by diffusion-controlled trapping relative to the water reaction (k_{HA}/k_w) is k_a/k_h, which depends only on the pK of the intermediate.

The importance of catalysis by hydrogen bonding is defined by the ratio of the rate constant for such catalysis, k'_{HA}, to the observed rate constant for the uncatalyzed reaction, k_0. For thiol addition, k_0 is given by

$$k_0 = \frac{k_1k_h}{k_h + k_{-1}} \qquad (24)$$

which reduces to $k_0 = k_1$ for the uncatalyzed addition reaction when a relatively stable intermediate abstracts a proton from water (k_h) faster than it reverts to reactants (k_{-1}) and reduces to $k_0 = k_w = k_1k_h/k_{-1}$ when the intermediate breaks down more rapidly and the proton transfer step becomes rate determining. Thus, for unstable intermediates (k_h rate determining) the observed rate constant k_0 is reduced below the rate constant of the attack step (k_1) by the factor k_h/k_{-1} and the ratio k'_{HA}/k_0 is correspondingly increased by the ratio k_{-1}/k_h.

For carbonyl addition reactions in general, there is an additional advantage, R, for catalysis by the hydrogen bonding mechanism when the addition intermediate is unstable that is directly proportional to the rate constant k_{-1} according to

$$R = \frac{k_{-1}}{k_h + k_s} \qquad (25)$$

The rate constant k_s refers to trapping of a dipolar addition intermediate $T^\pm$ to give T^0 through a solvent-mediated proton switch. When this mechanism of solvent-mediated trapping is available (e.g., in the addition of primary and secondary amines to the carbonyl group),[11] the rate of the background water reaction increases, with a corresponding decrease in the advantage of hydrogen bond catalysis relative to the uncatalyzed reaction. The addition of primary and secondary amines is less likely to exhibit catalysis by hydrogen bonding than the addition of anions for this reason and because the addition intermediate $T^\pm$ and the transition state for its formation are likely to be less basic for reactions of amines.

The relative importance of general acid catalysis by hydrogen bonding and by trapping, k'_{HA}/k_{HA}, is also directly proportional to the rate constant k_{-1} for breakdown of the addition intermediate, as shown in eq 26.

$$\frac{k'_{HA}}{k_{HA}} = \frac{k_{-1}}{k_{-a}}\,\text{antilog}\,[\alpha(15.74 - pK_{HA})] \qquad (26)$$

The ratio k'_{HA}/k_{HA} also depends on the stability of the hydrogen bond between the transition state and the catalyzing acid and this stability will increase with increasing strength of the acid according to some Brønsted coefficient, as shown in the right-hand term of eq 26. The derivation of eq 26 may be clarified by reference to Scheme II and the reaction coordinate diagram of Figure 9. The relative importance of the hydrogen bonding and trapping mechanisms is determined by the relative energies of the transition states for the k'_1 step for hydrogen bonding and for the k_a step for the trapping mechanism, when the acid is sufficiently strong that the k_a step is rate determining for proton transfer to T^- in the latter mechanism (Figure 9). This difference is most easily evaluated from

Table X. Factors Contributing to the Increased Importance of General Acid Catalysis by Cyanoacetic Acid with Weak Nucleophiles

Thiol	$k'_{HA}{}^{b}/k_0$, M^{-1}	Brønsted α	$\beta_{nuc}{}^{c}$	Relative contribution to the increase in catalytic advantage[a] from $k_{-1}{}^{d}$	$1/k_h{}^{e}$	Hydrogen[f] bonding
Methyl mercaptoacetate	0.4	0.13 ± 0.03	0.45	1	1	1
p-Methoxybenzenethiol	7.5	0.16 ± 0.03	0.51	38	2	2.6
3,4-Dichlorobenzenethiol	90	0.16 ± 0.03	0.52	97	3.2	2.6
p-Nitrobenzenethiol	500	0.19 ± 0.02	0.63	175	5.0	6.6
Pentafluorobenzenethiol	6600	0.26 ± 0.02	0.82	278	12	61

[a] Relative to the reaction with methyl mercaptoacetate. [b] Experimentally observed advantage for hydrogen bonding catalysis by cyanoacetic acid relative to 55.5 M water. [c] Calculated values of β_{nuc} for the hydrogen bonding mechanism catalyzed by water (k_1), estimated as described in the text. [d] Data from Table VIII. [e] k_h was obtained from pK_{TH} (method I, Table I) and $k_{-h} = 1 \times 10^{10}$ M^{-1} s^{-1} using eq 17. [f] Based on the quantity antilog $[\alpha(15.74 - pK_{HA})]$ for cyanoacetic acid.

the ratio of the rate constants in the reverse direction for breakdown of the intermediate in the presence of acid, k'_{-1}, and for separation of the T^-·HA complex, k_{-a}; i.e., the relative importance of the two pathways in the forward direction, k'_{HA}/k_{HA}, is given by the ratio k'_{-1}/k_{-a} for partitioning of the common intermediate through the two pathways in the reverse direction. If hydrogen bonding of HA to the intermediate and transition state provides no stabilization relative to water ($\alpha = 0$), the rate constants k_{-1} and k'_{-1} are equal and the breakdown of T^-·HA to reactants occurs with the barrier shown by the lower solid line in Figure 9. However, if the transition state of this breakdown reaction is stabilized by hydrogen bonding to HA (dashed line, Figure 9) this stabilization will depend on the pK of HA according to a Brønsted coefficient, α, and the ratio k'_{-1}/k_{-a} will show a corresponding increase according to

$$\frac{k'_{-1}}{k_{-a}} = \frac{k_{-1}}{k_{-a}} \text{antilog } [\alpha(15.74 - pK_{HA})] \qquad (27)$$

This equation does not include a term for the molarity of liquid water because it refers to the breakdown of T^- that is already hydrogen bonded to HA (k'_{-1}) or to water (k_{-1}). Thus, the advantage of the hydrogen bonding mechanism is given by eq 26.

The factors that contribute to the increasing importance of general acid catalysis by hydrogen bonding for the attack of weakly basic thiol anions on acetaldehyde are summarized in Table X for catalysis by cyanoacetic acid. The observed ratio, k'_{HA}/k_0, for cyanoacetic acid increases by a factor of more than 10^4, from 0.4 to 6600 M^{-1}, as the pK of the attacking nucleophile decreases from 7.8 to 2.7. Approximately 10^2 of this increase is caused by the decreased lifetime of the intermediate formed from the less basic thiols, as indicated by the rate constant k_{-1}. The values of k_{-1} for thiols of p$K < 7$ were estimated by extrapolating the Brønsted plots for catalysis by stronger acids to the pK of water to obtain $k_1/55.5$ and calculating k_{-1} from k_1 and the appropriate equilibrium constants (Table VIII). The experimentally determined value of $k_1/55.5$ falls close to the extrapolated Brønsted plot for general acid catalysis by hydrogen bonding for methyl mercaptoacetate (Figure 6). A small increase in k'_{HA}/k_0 of about tenfold may be attributed to a decreased value of k_h that results from the smaller basicity of the addition intermediate T^- formed from weakly basic thiols (Table VIII). Finally, there is an additional advantage on the order of 60-fold for the hydrogen bonding mechanism that is caused by the increase in the Brønsted coefficient α from 0.13 for methyl mercaptoacetate to 0.26 for pentafluorobenzenethiol. The combined advantages from these estimated contributions are slightly more than adequate to account for the observed increase in k'_{HA}/k_0.

The relationships between these mechanisms may be summarized as follows. When the intermediate breaks down to reactants faster than it is trapped by proton transfer involving solvent ($k_{-1} < k_h$) there *must* be catalysis by trapping. Catalysis by hydrogen bonding is also facilitated by a short lifetime of the intermediate (large k_{-1}) relative to both the background "water" reaction (eq 24) and to catalysis by trapping (eq 26). When catalysis by hydrogen bonding is faster than by trapping so that it is the observed mechanism ($k'_{HA} > k_{HA}$, $k'_{HA} > k_1k_a/k_{-1}$, and $k'_{-1} > k_{-a}$) it occurs by a preassociation mechanism in which the T^-·HA complex breaks down faster than it separates and the intermediates are not at equilibrium with the bulk solvent with respect to transport processes. In the absence of hydrogen bond stabilization a preassociation mechanism occurs only when the intermediate breaks down with a rate constant faster than the rate constant for diffusional separation of the T^-·HA complex,[5,29,30] usually about 10^{10}–10^{11} s^{-1}, but if there is significant stabilization of the complex and transition state by hydrogen bonding, the value of k_{-a} will be reduced and a preassociation mechanism can occur with values of k'_{-1} and k_{-1} of 10^9 s^{-1} or less (Table VIII). When the reaction is forced to proceed through a preassociation mechanism with an initial association of nucleophile, aldehyde, and acid in an encounter complex, *any* stabilization of the transition state by HA relative to water will result in an increase in the observed rate and catalysis by hydrogen bonding with $\alpha > 0$. If a preassociation mechanism is not enforced, k_1 rather than k_h will be rate determining for the "water" reaction, catalysis by HA must compete with catalysis by 55 M water, and a larger catalytic constant and α value are required in order for catalysis by hydrogen bonding to be significant. The preassociation mechanism causes a rate increase not only by hydrogen bonding to the transition state but also by placing a proton donor in position to rapidly protonate T^- as soon as it is formed and thereby *avoiding* the higher energy proton transfer step that involves rate-determining diffusion of relatively strong acids to the unstable intermediate T^-. In the reverse reaction it avoids the rate-determining diffusion away of HA from T^- with the rate constant k_{-a} and, as a consequence of this, the observed reaction rates with weak bases are larger than the rates of the overall process of proton abstraction from TH by weak bases through the Eigen mechanism.

In the special case in which catalysis at low acid concentration is by trapping and at high concentrations by hydrogen bonding, as in the methyl mercaptoacetate reaction, k_{HA} is larger than k'_{HA} (Figure 6), but catalysis by hydrogen bonding can be observed because of the change in rate-determining step at high acid concentrations. In this case there is significant catalysis by hydrogen bonding even when proton transfer is fast and the catalysis is not enforced through a preassociation mechanism. Thus, there is a small but significant stabilization of the transition state by hydrogen bonding (through k'_1) relative to the transition state for the uncatalyzed reaction (k_1) so that catalysis can be detected without the advantage described by eq 25. Such nonenforced catalysis has also been

observed for the addition of weakly basic carbanions[7] and of sulfite dianion[37] to the carbonyl group.

The rate constant of $k_{-1} = 5 \times 10^6\ s^{-1}$ for the expulsion of methylamine from **2**[36] is essentially the same as the rate con-

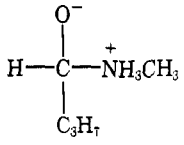

2

stant of $k_{-1} = 5.8 \times 10^6\ s^{-1}$ for the breakdown of T^- with expulsion of ethanethiol anion (Table VIII). This suggests that general acid catalysis of the addition of less basic amines should proceed through the same spectrum of mechanisms as with less basic thiol anions. Evidence for several of these mechanisms has already been reported by Sayer et al. for the addition of "α-effect" amines to substituted benzaldehydes.[5,6]

The results reported here establish that there is stabilization of the transition state by hydrogen bonding in the attack of certain thiol anions on carbonyl compounds, but do not rigorously establish whether or not the overall catalyzed reaction is stepwise or concerted; i.e., whether the reaction path proceeds through the intermediate species $T^-{\cdot}HA$ in a stepwise mechanism or proceeds directly on to $TH{\cdot}A^-$ through a concerted mechanism without passing through discrete steps or intermediates. The following evidence provides support for the stepwise reaction mechanism.

(1) The fact that T^- exists in water with a significant lifetime ($\gg 10^{-13}$ s) means that a concerted mechanism of catalysis is not enforced by a rate of expulsion of RS^- from T^- that is so fast that T^- does not exist and the reaction could not be stepwise.

(2) The water-catalyzed addition reaction certainly proceeds in a stepwise mechanism through T^- followed by a slow, thermodynamically unfavorable proton transfer and, since water falls on the Brønsted plot for general acid catalysis by hydrogen bonding, the same must be true for catalysis by other weak acids.

(3) Strong acids fall on the same Brønsted line as weaker acids and there is no evidence for an upward curvature of the Brønsted slope for strong acids, showing that there is no additional, lower energy reaction pathway that is different from the pathway followed by weak acids.

A concerted mechanism would be required if there were no barrier for proton transfer within the hydrogen bond so that the species $T^-{\cdot}HA$ cannot exist as an intermediate in a stepwise reaction mechanism. It is necessary that the basicity of the transition state be greater than that of water in order to obtain significant stabilization by hydrogen bonding to an acid HA and it is probable that the transition states have pK values in the range of roughly 2–9, as described in the following section. If there were a single potential well hydrogen bond with no barrier for proton transfer in these transition states, a thermodynamically favorable transfer of the proton would be expected to take place from strong catalyzing acids to the carbonyl oxygen atom in the transition state and the Bronsted coefficient α would approach 1.0 for the proton and other strong acids. Therefore, the fact that the observed values of α are all small means that there must be a barrier that prevents motion of the proton toward oxygen in the transition state. This would be expected if the proton is in one potential well of a double potential well hydrogen bond; the barrier could be caused by the presence of a water molecule between AH and the carbonyl oxygen atom. However, the possibility cannot be rigorously excluded that the barrier disappears for the more basic species T^- so that $T^-{\cdot}HA$ would not exist as a discrete intermediate when HA is a strong acid.

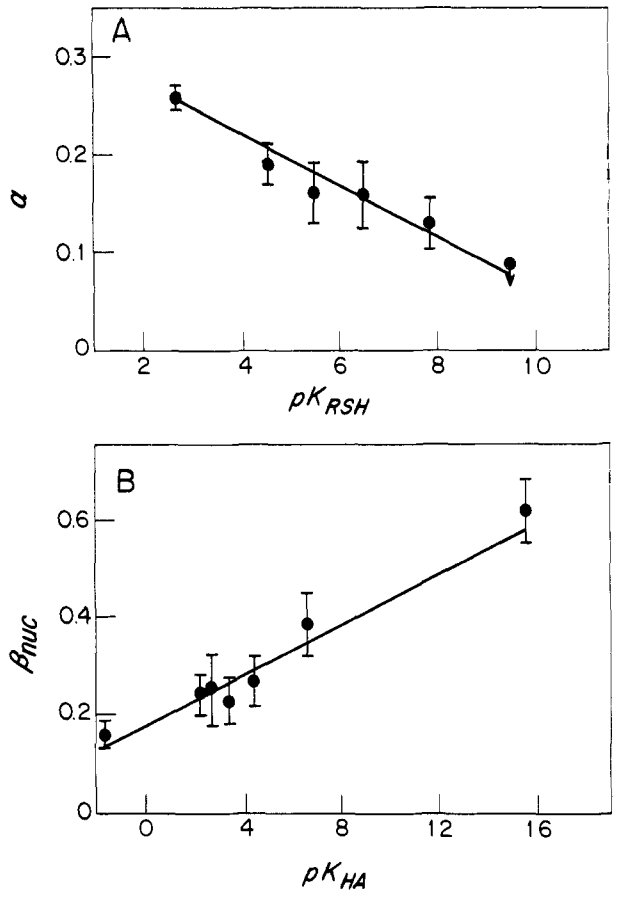

Figure 12. (A) Variation in α with the pK_{RSH} of the nucleophile. (B) Variation in β_{nuc} with the pK_{HA} of the acid catalyst. The solid lines have been drawn with a slope of $1/c_2 = 0.026$.

Structure–Reactivity Interactions. We consider here changes in the structure of the transition state for general-acid-catalyzed attack of thiol anions on acetaldehyde, as measured by changes in the Brønsted coefficient α and in β_{nuc}, with changing structure of the reactants and catalyst.

It is firmly established by the experimental data that the Brønsted coefficient α increases with decreasing basicity of the attacking thiol anion. No general acid catalysis is detectable for the attack of methoxyethanethiol anion. The absence of a rate increase in the presence of 1 M formate buffer,[2] 50% anion, sets an upper limit of $10^5\ M^{-2}\ s^{-1}$ on the rate constant for catalysis by formic acid and $\alpha \leq 0.09$ for the Brønsted coefficient for this reaction. General acid catalysis of the attack step is detectable with relatively strong acids for the less basic methyl mercaptoacetate anion (Figure 6, $\alpha = 0.13 \pm 0.03$) and exhibits increasing values of α as the basicity of the thiol anion decreases, with a value of $\alpha = 0.26$ for catalysis of the attack of pentafluorobenzenethiol anion (Table X).

This increase in α with decreasing pK_{nuc} of the attacking nucleophile can be described according to

$$\frac{\partial\alpha}{-\partial pK_{nuc}} = \frac{1}{c_2} = \frac{\partial\beta_{nuc}}{\partial pK_{HA}} \qquad (28)$$

with a Cordes coefficient[38] $1/c_2 = 0.026$ that is the slope of a plot of α against pK_{nuc} (Figure 12A). It is required by eq 28 that there be a corresponding increase in the sensitivity of the rate to the basicity of the attacking nucleophile, β_{nuc}, as the strength of the catalyzing acid decreases (pK_{HA} increases).

The dependence of the rate constants for catalysis by the proton, cyanoacetic and acetic acids, and water on the basicity of the nucleophile is shown in Figure 13. The observed rate constants have been corrected for catalysis by trapping and the

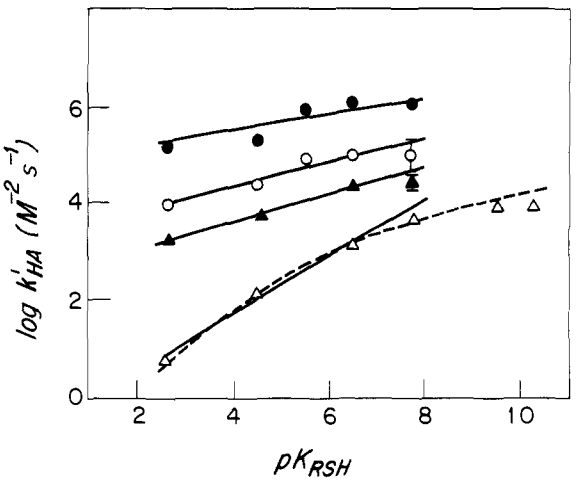

Figure 13. Dependence of the catalytic constants for the hydrogen bonding mechanism on the pK_{RSH} of the thiol. Catalytic constants for carboxylic acids have been corrected for catalysis due to trapping by subtracting the observed catalytic constant for boric acid and the catalytic constants for the proton have been corrected by subtracting ten times this catalytic constant. The catalytic constants k'_{HA}, for water were estimated from the intersection of the Brønsted plots at pK_{HA} = 16.0, except for ethanethiol and methoxyethanethiol anions for which $k'_{HA} = k_1/55.5$ M. The data are for catalysis by the proton (●); cyanoacetic acid (○); acetic acid (▲); and water (△). The solid lines are drawn with slopes given by the Cordes coefficient $1/c_2 = 0.026$. The dashed line is drawn as described in the text.

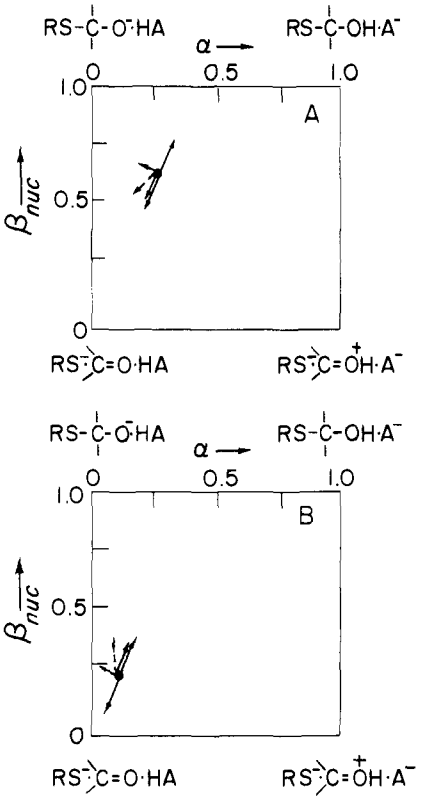

Figure 14. Reaction coordinate diagrams illustrating (A) the effect of increasing basicity of the nucleophile for the reaction of a weak nucleophile catalyzed by a weak acid and (B) the effect of decreasing acidity of the acid catalyst for the reaction of a strong nucleophile catalyzed by a strong acid.

points for water (k_1, Table VIII) are based on an extrapolation of the Brønsted plots obtained with stronger acids. Although there may be some curvature within the individual lines, it is clear that there is an increase in the slope, β_{nuc}, with increasing pK of the catalyst. The increase in β_{nuc} is consistent with the slope of $1/c_2 = 0.026$ (Figure 12B) and the data for thiols of pK = 2.6–7.8 are consistent with lines of slope 0.14, 0.24, 0.29, and 0.58 (Figure 13, solid lines) as required by eq 28 and the value of $1/c_2 = 0.026$. Figure 13 illustrates how the reciprocal relationships required by eq 28 follow directly from the experimental data with no assumptions about mechanism or transition state structure. The increasing slopes, β_{nuc}, with decreasing acid strength that are shown in the figure require that for a given series of catalyzing acids the range of rate constants, and hence the value of α, be smaller for a thiol of pK = 7.8 than for a thiol of pK = 2.6.

These results may be described in terms of the reaction coordinate diagrams of Figure 14 in which the horizontal and vertical axes are *defined* by the observed values of α and β_{nuc} and presumably represent some measure of the amount of proton transfer and of C–S bond formation, respectively. The energy contour lines are omitted from Figure 14 for clarity. Changes in the pK of the catalyst and nucleophile correspond to changes in the energy of the right edge and top edge of the diagrams, respectively, and such changes will shift the position of the transition state in a direction that is determined by the orientation and geometry of the saddle point and reaction coordinate.[39] The observed decrease in α with increasing basicity of the nucleophile corresponds to a shift in the position of the transition state to the left along the x axis. This shift can be accounted for if the reaction coordinate on the diagram has a significant horizontal component so that it is rotated clockwise from the vertical. Such a reaction coordinate, for the attack of a weak nucleophile catalyzed by a weak acid, is shown in Figure 14A. An increase in the basicity of the nucleophile lowers the energy of the top relative to the bottom of the diagram and shifts the position of the transition state in directions parallel and perpendicular to the reaction coordinate, as shown by the single-headed arrows. The resultant of these arrows, shown by the dashed arrow, requires a horizontal shift of the transition state to the left, corresponding to the observed decrease in α, and is consistent with a downward shift, corresponding to a decrease in β_{nuc}.

The corresponding diagram for the attack of a strong nucleophile catalyzed by a strong acid, shown in Figure 14B, serves to illustrate the effect of changing pK of the catalyst. A decrease in the acidity of the catalyzing acid raises the energy of the right relative to the left side of the diagram and shifts the position of the transition state in directions parallel and perpendicular to the reaction coordinate, as shown by the vectors. The resultant shift in the position of the transition state corresponds to an upward motion, leading to the observed increase in β_{nuc}, and does not require any horizontal shift that would correspond to a change in α. The Brønsted line in Figure 8 for acids of pK = −1.7 to 9 and the lower line in Figure 6, for catalysis by hydrogen bonding, give no evidence for a change in α with changing pK of the acid and are inconsistent with any large change. These shifts in the position of the transition state are consistent with a direction of the reaction coordinate that is rotated by only a moderate amount from the vertical, with a relatively small downward curvature along the reaction coordinate and a steeper upward curvature perpendicular to the reaction coordinate. This is what might be expected for a hydrogen-bonded transition state in which the proton is in a potential well that moves to the right as the transition state becomes more basic and approaches the structure of the anionic addition intermediate T^-.

The data also suggest that the value of β_{nuc} increases with decreasing basicity of the attacking thiol anion; this may be described as a "Hammond–Marcus" effect.[39] The value of β_{nuc} is 0.1 ± 0.1 for the attack of basic, aliphatic thiol anions on acetaldehyde[2] and is ~0.6 for the attack of weakly basic, aromatic anions in a "water" reaction (Figure 13). The data are not adequate to determine whether there is curvature within the series of aromatic thiol anions. The slower attack of thiol

anions on esters and thiol esters exhibits a value of $\beta_{nuc} = 0.3$ with no indication of any difference between aliphatic and aromatic thiols;[23] however, the data do not completely exclude the possibility that β_{nuc} is larger for the aromatic thiol anions. A decrease in β_{nuc} with increasing basicity of the nucleophile corresponds to a downward movement of the transition state in Figure 14. Such a shift is consistent with a large vertical component to the reaction coordinate and a smaller curvature in the parallel than in the perpendicular direction to the reaction coordinate, as suggested above, so that a decrease in the energy of the top relative to the bottom edge of the diagram shifts the transition state downward in a direction that is predominantly parallel to the reaction coordinate. The change in β_{nuc} with increasing basicity of the nucleophile is described, within experimental error, by a coefficient $p_y = \partial\beta_{nuc}/-\partial pK_{nuc} = 0.089$, as shown by the dashed line in Figure 13. This dashed line, for hydrogen bonding catalysis by water, is drawn according to

$$\log k'_{HA} = 2.75 + 0.64pK_{RSH} - 0.3pK_{HA} + 0.026pK_{HA}pK_{RSH} - 0.089pK^2_{RSH}/2 \quad (29)$$

in which the coefficient of the last term is $\partial\beta_{nuc}/-\partial pK_{RSH}$. The coefficient of the fourth term represents the Cordes coefficient, $1/c_2$, and the coefficients of the other terms are defined by the intercepts of the Cordes plots in Figure 12. Equation 29 also predicts curvature of the lines for catalysis by other acids in Figure 13, but the data are not of sufficient accuracy to determine the presence or absence of such curvature. These structure-reactivity relationships are utilized to define an energy surface for the reaction in the accompanying paper.[39]

A transition state with increased S-C bond formation will have an increased negative charge and basicity on the carbonyl oxygen atom that will give a correspondingly stronger hydrogen bond to the catalyzing acid. The increase in hydrogen bond strength is expected to follow some relationship such as that proposed by Hine[40] (eq 30 and 31)

$$\log K_{AB} = \tau(pK_{HA} - pK_{H_2O})(pK_{H_3O^+} - pK_{BH}) - 1.74 \quad (30)$$

$$-\alpha = \frac{\log K_{AB} + 1.74}{pK_{HA} - pK_{H_2O}} = \tau(pK_{H_3O^+} - pK_{BH}) \quad (31)$$

in which K_{AB} corresponds to the ratio of the rate constants for catalysis by an acid of pK_{HA} and by water (k_1), pK_{BH} is the pK of the conjugate acid of the transition state, and τ is a constant taken as equal to 0.024. Substitution of the observed values of α into eq 31 gives pK_{BH} values for the transition state that increase from <2.0 to 9.1 as the pK of the attacking thiol decreases from $pK = 9.5$ to $pK = 2.7$. If it is assumed that the pK of protonated acetaldehyde is -3.0[41] and that the pK of the transition state increases linearly with β_{nuc} to the pK of the product hemithioacetal (Table I) the values of β_{nuc} may be calculated from the pK_{BH} values of the transition state. The resulting values of β_{nuc} increase with decreasing basicity of the thiol, from ≤0.32 for ethanethiol anion to 0.82 for pentafluorobenzene thiol anion. The calculated values of β_{nuc} in Table X are consistent with the slopes of lines tangent to the dashed line in Figure 13 at the pK values of the individual thiols. These calculations are obviously too crude to provide a quantitative description of the reaction, but they do serve to illustrate that the changes in α and β_{nuc} with changing structure of the reactants are not unreasonable and may be described in terms of the behavior that might be expected for a hydrogen-bonding mechanism.

References and Notes

(1) This work was supported by grants from the National Institutes of Health (GM 20888) and the National Science Foundation (GB-31740). H.F.G. is a postdoctoral fellow of the American Cancer Society (PF-1111).
(2) G. E. Lienhard and W. P. Jencks, *J. Am. Chem. Soc.*, **88**, 3982 (1966).
(3) R. E. Barnett and W. P. Jencks, *J. Am. Chem. Soc.*, **91**, 6758 (1969).
(4) R. G. Kallen, personal communication.
(5) J. M. Sayer and W. P. Jencks, *J. Am. Chem. Soc.*, **95**, 5637 (1973).
(6) S. Rosenberg, S. M. Silver, J. M. Sayer, and W. P. Jencks, *J. Am. Chem. Soc.*, **96**, 7986 (1974).
(7) W. N. White and W. P. Jencks, in preparation.
(8) W. R. Abrams and R. G. Kallen, *J. Am. Chem. Soc.*, **98**, 7777 (1976).
(9) W. P. Jencks, *Acc. Chem. Res.*, **9**, 425 (1976).
(10) W. P. Jencks and H. F. Gilbert, *J. Pure Appl. Chem.*, **49**, 1021 (1977).
(11) A. C. Satterthwait and W. P. Jencks, *J. Am. Chem. Soc.*, **96**, 7031 (1974).
(12) G. L. Ellman, *Arch. Biochem. Biophys.*, **82**, 70 (1959).
(13) A. A. Frost and R. G. Pearson, "Kinetics and Mechanism", 2nd ed, Wiley, New York, N.Y., 1961.
(14) V. Gold, "pH Measurements", Wiley, New York, N.Y., 1956, p 119.
(15) R. P. Bell, M. H. Rand, and K. M. A. Wynne-Jones, *Trans. Faraday Soc.*, **52**, 1093 (1956).
(16) J. L. Hogg, D. A. Jencks, and W. P. Jencks, *J. Am. Chem. Soc.*, **99**, 4772 (1977).
(17) L. Pentz and E. R. Thornton, *J. Am. Chem. Soc.*, **89**, 6931 (1967).
(18) W. P. Jencks and K. Salvesen, *J. Am. Chem. Soc.*, **93**, 4433 (1971).
(19) E. Hand and W. P. Jencks, *J. Am. Chem. Soc.*, **97**, 6221 (1975).
(20) J. L. Hogg and W. P. Jencks, *J. Am. Chem. Soc.*, **98**, 5643 (1976).
(21) H. F. Gilbert, *J. Chem. Educ.*, **54**, 492 (1977).
(22) M. Eigen, *Angew. Chem., Int. Ed. Engl.*, **3**, 1 (1964).
(23) D. Hupe and W. P. Jencks, *J. Am. Chem. Soc.*, **99**, 451 (1977).
(24) These rate constants and the value of k_h in Table VIII are smaller than the values reported in preliminary communications[9,10] because the latter values were obtained from an estimated value of pK_{TH} which is larger than the experimental value that was obtained in this work (Table I) and the average value of k_{-h} is smaller than the value of 10^{10} M^{-1} s^{-1} used for the preliminary estimation.
(25) R. P. Bell and P. G. Evans, *Proc. R. Soc. London, Ser. A*, **291**, 297 (1966). The values of $p = 2$ and $q = 4$ were used for boric acid since the acid–base reaction involves a water molecule[27] $(HO)_3B{:}OH_2 \rightleftharpoons B(OH)_4 + H^+$ with two equivalent acid sites in the forward direction and four equivalent basic sites in the reverse reaction.
(26) J. A. Ball, E. Grunwald, and E. Hayon, *J. Am. Chem. Soc.*, **97**, 2995 (1975).
(27) R. P. Bell, J. O. Edwards, and R. B. Jones in "The Chemistry of Boron and Its Compounds", E. L. Muetterties, Ed., Wiley, New York, N.Y., 1967, p 209.
(28) R. W. Taft, D. Gurka, L. Joris, P. von R. Schleyer, and J. W. Rakshys, *J. Am. Chem. Soc.*, **91**, 4801 (1969).
(29) W. P. Jencks and K. Salvesen, *J. Am. Chem. Soc.*, **93**, 1419 (1971).
(30) L. D. Kershner and R. L. Schowen, *J. Am. Chem. Soc.*, **93**, 2014 (1971).
(31) A. Kankaanperä and P. Salomaa, *Acta Chem. Scand.*, **23**, 712 (1969); A. Kankanperä and R. Aaltonen, *Suom. Kemistil. B*, **43**, 183 (1970). However, the rate constant for protonation of tris(*p*-nitrophenyl)methane anion by boric acid in alcohol is only slightly abnormal, based on its pK in water (G. N. Lewis and G. T. Seaborg, *J. Am. Chem. Soc.*, **61**, 1894 (1939)).
(32) R. P. Bell, D. H. Everett, and H. C. Longuet-Higgins, *Proc. R. Soc. London, Ser. A*, **186**, 443 (1946); M. L. Bender and A. Williams, *J. Am. Chem. Soc.*, **88**, 2502 (1966).
(33) D. M. Goodall and F. A. Long, *J. Am. Chem. Soc.*, **90**, 238 (1968).
(34) B. R. Glutz and H. Zollinger, *Helv. Chim. Acta*, **52**, 1976 (1969).
(35) S. L. Johnson and D. L. Morrison, *J. Am. Chem. Soc.*, **94**, 1323 (1972).
(36) J. Hine, J. C. Craig, Jr., J. G. Underwood II, and F. A. Via, *J. Am. Chem. Soc.*, **92**, 5194 (1970).
(37) P. R. Young and W. P. Jencks, *J. Am. Chem. Soc.*, **99**, 1206 (1977).
(38) E. H. Cordes and W. P. Jencks, *J. Am. Chem. Soc.*, **84**, 4319 (1962); W. P. Jencks, *Prog. Phys. Org. Chem.*, **2**, 63 (1964); L. do Amaral, W. A. Sandstrom, and E. H. Cordes, *J. Am. Chem. Soc.*, **88**, 2225 (1966).
(39) D. A. Jencks and W. P. Jencks, *J. Am. Chem. Soc.*, following paper in this issue.
(40) J. Hine, *J. Am. Chem. Soc.*, **93**, 3701 (1971).
(41) The pK of the conjugate acid of acetaldehyde is assumed to be similar to the value of −2.8 reported for acetone by E. M. Arnett and G. Scorrano, *Adv. Phys. Org. Chem.*, **13**, 84 (1976).